Biodegradable Sulfated Dendritic Nanocarriers for Biomedical Applications

Inaugural-dissertation

to obtain the academic degree

Doctor Rerum Naturalium (Dr. rer. nat.)

submitted to the Department of Biology, Chemistry and Pharmacy

of Freie Universität Berlin

by

Magda Ferraro

From Vicenza, Italy

2019

The following project was carried out within the research group of Prof. Dr. Rainer Haag from **January 2016** until **May 2019** at the Institute of Chemistry and Biochemistry of the Freie Universität Berlin.

1. Reviewer: Prof. Dr. Rainer Haag, Freie Universität Berlin
2. Reviewer: Dr. Jens Dernedde, Charité Universitätmedizin Berlin

Day of defense: 02.07.2019

To my parents

Acknowledgements

First of all, I would like to thank Prof. Dr. Rainer Haag for giving me the possibility to conduct my doctoral studies in his group, being my supervisor und supporting me through these years.

I would also like to thank Dr. Jens Dernedde for being the 2nd supervisor of this thesis and a mentor, and for his precious advice in the scientific field.

I would like to thank the BCP Core Facility BioSupramol for the numerous measurements and in particular Dr. Andreas Schäfer for his explanation on controversial NMR.

Dr. Emanuel Fleige and Dr. Florian Paulus are kindly thanked for the support and the great time they offered me during my Erasmus, which also motivated me to proceed with my studies in this groups and on this topic.

Kim Silberreis, Dr. Priyanka Ray, and Dr. Ehsan Mohammadifar are kindly thanked for being great cooperation partners, for being always willing and reliable, for sharing the bad and great moments that led to the publications of our manuscripts.

A special thank goes to Dr. Wiebke Fischer, for her support in every stage on my studies at the FU, to Jutta Hass and Eike Ziegler for the handling of the bureaucratic matters, to Lisa Hummel for taking care of my scholarship bureaucracy.

I would like to thank Dr. Nadine Rades and Daniel Braatz for the proof-reading of this thesis, and Dr. Pamela Winchester for the linguistic revision of my manuscripts and thesis. Moreover, I would like to thank Alexander Oehrl for the numberless corrections to my documents in German, that helped me in improving my knowledge and handling of the language.

The Haag family is thanked for the pleasant time, especially the lunch group for the great non-working time and experiences. I'm grateful to my lab-mates Alexander Oehrl, Dr. Ehsan Mohammadifar, Maiko Schulze, Dr. Svenja Ehrmann, Daniel Braatz, Dr. Leonhard Urner, and Dr. Katharina Huth for the friendly atmosphere, which was present every day in the lab, for their support, for the scientific discussions, and for rendering every day a positive one.

Ehsan is thanked not only for being a good colleague but first of all for being a good friend, almost like a brother, for sharing with me his knowledge and making me laugh every time I was down.

A special friendship developed thorough these years with Alexander Oehrl and Dr. Era Kapourani. We had great moments at work and in our private life, and I am sincerely thankful to have met you.

I would like to thank Beatrice Battistella for her endless e-mail, which opened the way for a fantastic friendship. I am thankful for the great time we had together.

I would like to thank my families, the Italian one which was always present despite the 1000 km distance, and the German one, which made me feel home again. It's hard to find the words to describe how thankful I am to my parents, for their trust in me, their support, their strength, and the motivation they have given to me during these years.

Finally, I want to thank Patrick Beuckmann for the patience he shared with me during my studies, for his love and support, which helped me to not give up. I am looking forward for the next chapter that we are going to write together.

Table of Contents

1 Introduction

Inflammation is a common denominator of various pathologies, ranging from arthritis to Alzheimer, including heart diseases and even cancer.[1–3] Cancer is one of the diseases with the highest mortality rates and it is diagnosticated with increasing incidence. The extreme heterogeneity of the pathologies, even of those that belong to the same family, renders their treatment arduous and challenging. Even though numerous drugs have been developed and new ones are under investigation, failure in the therapeutic effect is often experienced *in vivo*, due to the low efficacy of drugs, their poor bioavailability, and the continuous evolution of the diseases, which can develop their own surviving strategies. The investigation of the illnesses and the development of new strategies for their treatment is nowadays of primary interest, not only for medicine, but it is also a crucial aspect for the natural sciences, like biology and chemistry. The joint efforts of scientists from different fields could be the key for new therapeutic approaches using innovative drug delivery systems.

1.1 Dendritic nanocarriers for drug delivery

1.1.1 Drug delivery

The treatment of diverse illnesses is based on the use of drugs, which are generally small molecular weight hydrophobic compounds. Diverse administration pathways can be employed, which are classified as enteral (oral, sublingual, and rectal), parenteral (intravenous, intramuscular, and inhalation), and topical (through the skin).[4,5]

After the administration, drugs are usually distributed in the whole body, but only a small amount reaches the desired site of action. Moreover, due to their size, drugs exhibit short surveillance in the blood stream and commonly undergo rapid renal and hepatic clearance. Diffusion in the healthy tissue can easily happen, provoking undesired side effects. As result, only a restrained amount of the active principle dispensed will perform the desired activity and repeated administration of the medicines is required.[6] Besides the discomfort for the patient to repeat the treatment, uncontrolled administration of drugs can lead to the overdosage and can provoke increased side effects up to poisoning.

In order to overcome these problems, researchers have spent a lot of effort to develop formulations capable of enhancing drug's efficacy, known as drug delivery systems (DDS). The primary aim of DDS is to improve the solubility and the circulation time of drugs. Moreover, the

delivery systems can be developed to release the drugs in a controlled manner over time, therefore avoiding the necessity of repeated administrations. Finally, the possibility to target desired site of action, reducing the release in the healthy tissue, can also be achieved.[7]

For the development of DDS both organic and inorganic materials, ranging from natural and synthetic polymers to metal-based ones, can be employed.[8] The main characteristic shared by these compounds is the size, which is generally in the range 1-100 nm. For that reason, those systems are also called nanomaterials and find application in the field of nanomedicine.[9,10]

Concerning the employment of polymeric biomaterials, a suitable macromolecule, that serves as a vector is needed. Generally, this exhibits a hydrophilic character to enhance the water solubility of the drug, is biocompatible, and can be eliminated by the organism when the carrier's action has been accomplished.[11]

The first report of this arrangement was published in 1975 by Ringsdorf and nowadays it is known with the name of the "Ringsdorf model."[12] In this report, a small drug is covalently linked to the polymeric backbone, forming a polymer-drug conjugate.

For the release of the active compound from the conjugate, the presence of a labile linker in between the polymer and the drug is required. Possible linkers and strategies to induce the release will be discussed in more detail in the chapter on stimuli-responsive nanocarriers (Chapter 1.3.3.).

Based on the Ringsdorf model, diverse systems constructed on polymers have been established for the delivery of therapeutic agents, which are also termed polymer therapeutics.

Generally, this approach is chosen for the conjugation of small drugs, proteins and antibodies. One of the mostly used polymers for such conjugations is poly(ethylene glycol) (PEG), a hydrophilic and biocompatible polyether, which is already present in many medical formulations, as approved by the Food and Drug Administration (FDA). PEG is often coupled to proteins, as it is an effective shielding agent and prevents the rapid clearance from the blood stream.[13] However, in the recent years, numerous papers have shown the possible toxicity of PEG, mostly because of its lack in biodegradability and its immunogenicity, and alternatives to PEGylation are therefore under investigation.[14,15]

The first PEGylated enzyme on the market, Adagen®, was approved in the 90s. Since then, numerous other polymer therapeutics have entered the market. More are in the clinical development, including antibodies, growth factors and cytokines.[16]

Besides the covalent attachment of the drug to the polymeric scaffold, it is also possible to construct nanocarriers in which the guests are physically entrapped. This approach is based on the establishment of hydrophobic, electrostatic, or hydrogen-based interactions between the host and the guest, resulting in the so-called supramolecular complexes.[17,18] Already at the beginning of the

90s, Newcome and coworkers observed the formation of unimolecular micelles using dendrimers and could demonstrate the encapsulation of spectrophotometric guests in the interior.[19] Furthermore, in 1994 Meijer and coworkers also reported on the use of the internal cavities of dendrimers to entrap guest molecules, and named it "dendritic box."[20] On this basis, the possibility to entangle a drug inside of the micelles has been investigated. In particular, copolymers, which bear both a hydrophobic and a hydrophilic chain, can assemble to micelles. By tuning the characteristics of the hydrophobic part forming the core, it is possible to enhance the interaction with different kinds of guest molecules, ranging from drugs to genetic material.[21] Besides the amphiphilic block copolymers, another approach for the transport of guest molecules involves the formation of unimolecular micelles. Such core-shell architectures are composed of a single molecule and therefore do not disassemble as classical micelles upon dilution or application of external forces.[22] A comparison of the two approaches is presented in Figure 1.

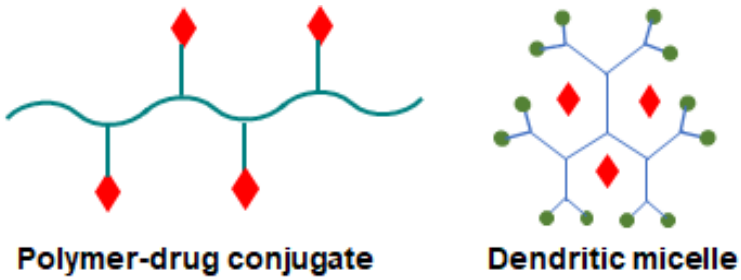

Figure 1. Schematic representation of a polymer-drug conjugate and a dendritic core-shell architecture acting as a unimolecular micelle, loaded with a drug (in red).

1.1.2 Dendritic and hyperbranched polymers

Dendritic polymers are macromolecular highly branched compounds, whose name is derived from the Greek word "dendron," as the structure resembles that of a tree. Four main examples of them are dendrimers, dendrons, dendronized polymers, and hyperbranched polymers, which are exemplified in Figure 2.

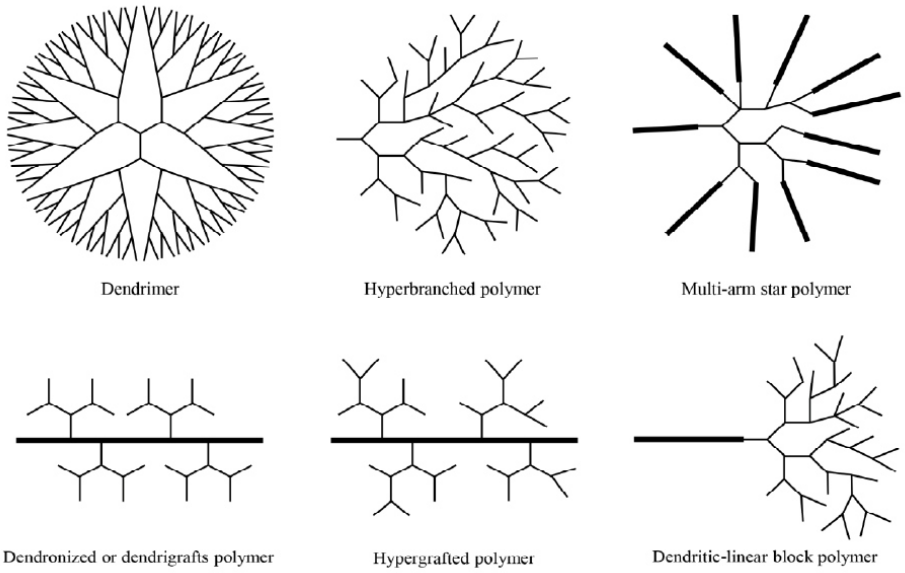

Figure 2. Structure of dendrons, dendritic, and hyperbranched polymers. Reprinted with permission from Ma et al.[23] (Copyright 2016, Ivyspring International Publisher)

Dendrimers present a perfectly branched architecture, which is defined monodisperse if the polydispersity index (PDI) is equal to one. The same is true for dendrons, which are composed of one branch of a dendrimer.

On the contrary, polymers are polydisperse. This is the case of dendronized and hyperbranched polymers. To obtain dendronized polymers, dendrons are usually attached to linear scaffolds. Dendrimers are generally obtained via a multi-step process, while the less defined hyperbranched architectures are more easily accessible via polymerization.[24]

Dendrimers were firstly parallelly synthesized in the 80s by Vogtle and Tomalia, who developed the first poly(propylene imine) (PPI) and poly(amido amine) (PAMAM) dendrimer respectively. Almost contemporary, the Newkome group also reported on dendrimers, but under the name of “arborols."[25]

In dendrimers three main domains are generally present: (i) a central core, (ii) branching arising from the core, which present a repeating structure and are geometrically ordered to form a radial development called “generation,” and (iii) terminal units, which can be used for further functionalization.[26]

To obtain these perfect symmetric structures two approaches are generally employed, named divergent and convergent. In the first case, the functional groups of the core are activated and reacted with the branching monomer units. In the second case, the approach is inverted. Once the branching units are complete, they are attached to the focal point. The PAMAM dendrimer

synthesized by Tomalia et al. is an example of the divergent approach, while the convergent one was initially explored by Frechet and Hawker, resulting in a poly(benzylether).[27,28]

Due to their perfect structure, dendrimers find many applications in the biomedical field and, in particular, as nanocarrier molecules. The capacity of dendrimers to enhance the solubility of hydrophobic drugs for anti-inflammatory and anti-tumoral applications has extensively been investigated.[29,30]

VivaGel® is an example of commercially available topical antimicrobial based on a dendrimer that acts as a drug itself. It is based on lysin and present a polyanionic surface which can bind to HIV and herpes simplex virus (HSV) surface in a multivalent fashion.[31]

PAMAM dendrimers find application, for example, in the field of gene delivery, as cationic polymers are needed for the delivery of DNA.[32] Moreover, PAMAM dendrimers functionalized with end-groups such as pyrrolidone exhibit fluorescence and can therefore also be used in the field of imaging.[33,34] Cationic dendrimers based on PAMAM and poly(propylene imine) (PPI) reacted with alkyl epoxide to induce an hydrophobic character were able to deliver siRNA to the lung epithelium.[35]

Polyester-based dendrimers with enhanced water solubility have been demonstrated to be promising scaffolds for the delivery of anticancer drugs.[36] Moreover, PEGylated biodegradable dendrimers have shown a prolonged circulation time in the blood stream in conjunction with a restrained release of the guest in the healthy tissue.[37]

As already mentioned, the less perfect architecture of hyperbranched polymers in comparison to that of dendrons renders them easily accessible from a synthetic point of view. Moreover, while the generation and size of dendrimers is generally constrained, hyperbranched systems do not present this limitation.

The first description of hyperbranched polymers is related to the synthesis of resins using tartaric acid (A_2B_2 monomer) and glycerol (B_3 monomer) operated by Berzelius.[38] This was lately followed by a theoretical study from Flory,[39] where hyperbranched systems were postulated via the multistep polycondensation of AB_2 type monomers. Nowadays, different synthetic approaches, not only involving the AB_x type monomers, can be used to produce hyperbranched polymers. The polymerization of $A_2 + B_y$ monomers, ring-opening multibranching polymerization (ROMB), and self-condensing vinyl polymerization (SCVP) are just few examples of them.[40] Regardless of the chosen approach, all hyperbranched systems are characterized by the so-called degree of branching (DB), which defines the ratio of branching and terminal units with respect to the possible ones.[41] In comparison to the perfect dendrimers, which possess a DB of 100%, hyperbranched polymers can

usually maximally achieve a DB of 40-60%. For the calculation of the DB, diverse equations can be applied, based on the molecular weight of the polymer under consideration.[42]

Due to their straightforward synthesis and easy functionalization, hyperbranched polymers find numerous applications in technical biological fields. Some exemplary hyperbranched polymers are shown in Figure 3.

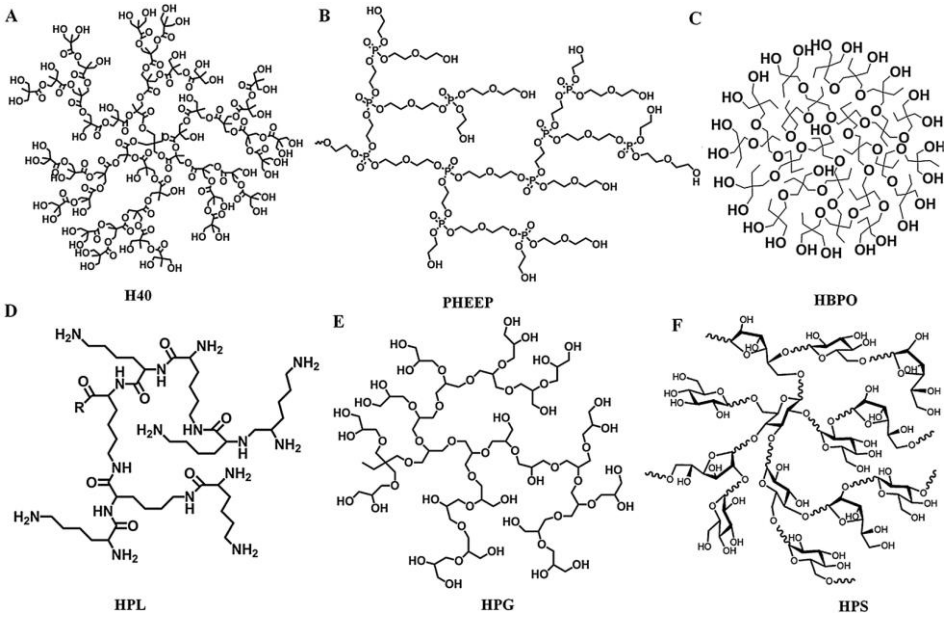

Figure 3. Examples of biocompatible hyperbranched polymers. (A) Polyester, (B) polyphosphate, (C) poly(3-ethyl-3-oxetanemethanol), (D) polylysine; (E) polyglycerol, and (F) polysaccharide. Reprinted with permission from Wang et al.[43] (Copyright 2015, Royal Society of Chemistry).

Boltorn™ H40 is an example of the 4th generation polyester with 2,2-bis(methylol)propionic acid (bis-MPA) branching units. As probably one of the most successful examples of polyester, the properties of Boltorn have been investigated by numerous groups, concerning the structure, the rheological properties, and its suitability as carrier for drug delivery.[44,45]

Polyphosphates show good biocompatibility, as the hydrolysis and the enzymatic degradation lead to low molecular weight products. Polymers based on 2-(2-hydroxyethoxy)ethoxy-2-oxo-1,3,2-dioxaphospholane (HEEP) have been shown to be suitable nanocarriers both for the development of drug-conjugates and self-assembled systems like micelles, and to be capable of releasing the payload.[46,47]

In the multitude of branched polymers which have been studied, hyperbranched poly(glycerol) (hPG) has emerged as a promising and versatile structure. It is also called dendritic poly(glycerol) (dPG) (labelled in Figure 3 as HPG). Perfect monodisperse poly(glycerol)s are also spherically available. Due to its dendrimer-like, ether-based structure, and the presentation of

multiple hydroxyl groups, this polymer has a high-water solubility and low viscosity. It is chemically stable and shows a good biocompatibility and low toxicity. It can be synthesized on multigram scale, with accessibility to a broad range of molecular weights and PDIs.[48]

The first synthetic report of hPG is from Sandler and Berg, in the 60s.[49] In this study, glycidol was polymerized at room temperature and the effect of diverse catalysts was investigated in comparison to the reactivity of propylene oxide. Generally, glycidol exhibited a marked tendency to polymerize in comparison to propylene oxide, and similar molecular weights were obtained using the different catalysts. Further studies have led to the development of the cationic ring-opening polymerization of glycidol in the presence of acid catalysts.[50,51] The main limitation of this process is, however, the accessibility of high molecular weight, due to the low control over the reaction, as side reactions and chain termination can easily happen. The main products of this synthetic approach are usually oligomers. The great interest of the scientific community in this polymer has led finally to the development of the anionic ring-opening multi-branching polymerization. In an approach with controlled monomer addition and the deprotonation of the initiator, it was possible to favor molecular weights up to 20 kDa and to maintain a narrow PDI under 1.5.[52] Higher molecular weight hPGs, up to 100 kDa, were reported by Moore et al., using low molecular weight hPG as a macroinitiator.[53] The straightforward synthetic approach and the possibility to obtain the product on a kilogram scale have rendered hPG a versatile alternative to dendrimers for the use in biomedical applications. In our group, we have developed a quite wide expertise on hPG-based drug delivery systems. We have mainly focused on delivery platforms such as nanogels, polymeric nanoparticles, and core-multishell (CMS) nanoparticles for applications which range from topical delivery[54–58] to gene and siRNA delivery[59], and also the delivery of anticancer drugs.[60–62]

1.1.3 Biodegradable polymers

The necessity to develop synthetic biomaterials which can undergo degradation is of great interest for diverse branches of the industry, and particularly crucial for biomedical applications. Together with this, the biocompatibility and the degradation to non-toxic byproducts are essential characteristics of polymer for *in vivo* applications.

The process of biodegradation is essentially composed of two steps: at first, the polymer chain is broken down to smaller fragments (depolymerization), which can be then transported into the cells and be assimilated. In order to ensure the degradation, hydrolysable bonds in the polymer have to be present. The hydrolysis can either be chemically or enzymatically catalyzed. Furthermore, characteristics such as the hydrophilicity or hydrophobicity of the compound, its

flexibility or stiffness, the size, and the stability to environmental factors play also a role in the degradation of the compound.[63] As an example, regular chains enhance the crystallinity of the materials and can therefore hinder the degradation via enzymatic attack. Hydrolytic enzymes are represented by lipase, esterase, proteases, and others.

As in many aspects of every-day life, nature can help to understand the dynamic of these compounds, as it offers numerous examples of biodegradable polymers, such as polysaccharides and proteins. Collagen, one of the most abundant mammalian proteins, and chitosan, a natural polysaccharide, have found application in drug delivery.[64] Even though natural polymers are an interesting source of inspiration and have found some applications as biomaterials, the low control on the structure and on the mechanical properties still represent limitations to their employment. Therefore, synthetic compounds have been developed, which can overcome these disadvantages.

Polyesters are a class of biodegradable polymers widely employed, which present ester bonds in the backbone and can therefore be hydrolyzed both by water and by the action of enzymes (Figure 4).

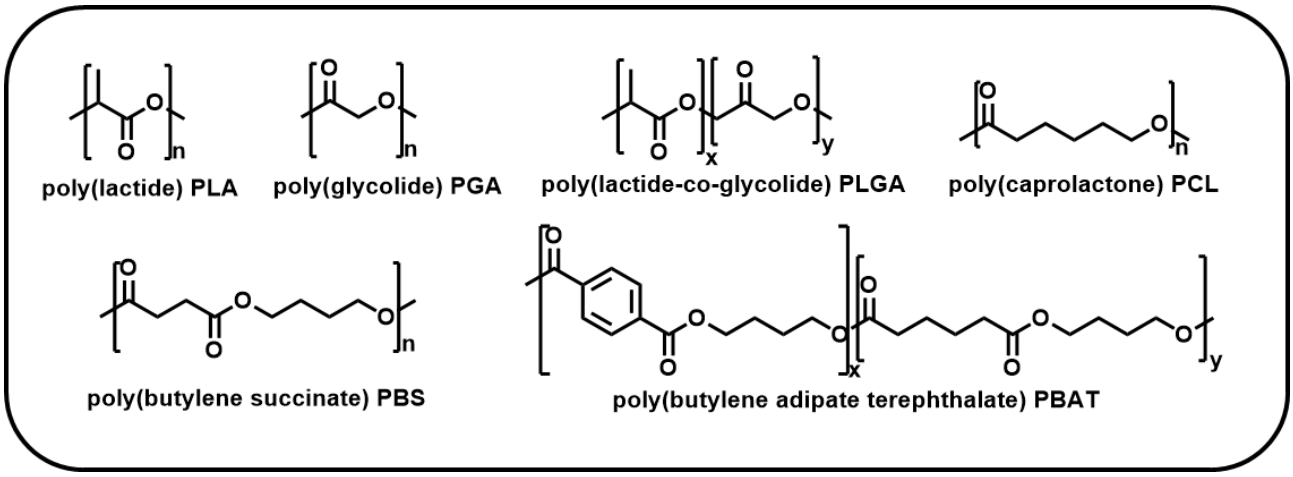

Figure 4. Examples of biodegradable polyesters.

Poly(lactide) (PLA) and poly(glycolide) (PGA), for example, find numerous applications in the biomedical field, as their degradation leads to the production of lactic acid and glycolic acid and are therefore FDA-approved.[65] The copolymerization of these results in one of the most used polymer for drug delivery application: poly(lactide-co-glycolide) (PLGA).[66,67]

Another interesting aliphatic polyester is poly(caprolactone) (PCL), whose much lower degradation rate *in vivo* renders the polymer also suitable for the development of implants and long term applications.[68] Recently, Jeong and coworkers have reported the synthesis of "fast degradable polycaprolactone": to improve the degradation rate, oxalate was employed for connecting the chains of oligocaprolactone. The polymer was used for the encapsulation of paclitaxel. *In vivo* release

studies showed a performance comparable to that of a PLGA-based nanocarrier. The complete clearance from the body was in two months.[69]

Poly(butylene succinate) (PBS) has been studied in combined materials together with PEG or chitosan for the application in tissue regeneration and engineering, but the high hydrophobic character of the material still represents a limitation to its employment.[70] To reinforce the strength of the polyester, the incorporation of aromatic moieties such as in poly(butylene adipate terephthalate) is a suitable strategy.[71]

Other examples of polymers which can be degraded by hydrolysis and are therefore labelled as biodegradable, are the polyanhydrides, the polyphosphazenes, and the polyacetals (Figure 5).

Polyanhydrides are also a class of FDA-approved compounds for the delivery of drugs, due to their rapid degradation to the corresponding diacid. Moreover, polyanhydrides are inexpensive and have straightforward synthetic approaches, tunable structures and predictable degradation rates.[72] Polyanhydrides are extremely sensitive to hydrolysis and must be stored at low temperatures before usage, in order to prevent their premature degradation. This drawback has, however, become the strength and motivation to develop medical electronic devices, like batteries which melt in the body or transient electronics which disappear completely in restrained time.[73]

Polyphosphazenes are hybrid materials with an inorganic backbone composed of phosphorus and nitrogen, which usually have organic substituents. Water soluble polyphosphazenes have been studied as vaccine adjuvant and as carrier for drug delivery.[74] Moreover, diverse polyphosphazenes have been investigated for tissue engineering, such as scaffold for bones, or as coating for materials in contact with blood.[75] Peptide-grafted polyphosphazenes have been reported, in which the sequence Gly-Phe-Leu-Gly (GFLG) was attached to the inorganic scaffold to obtain an enzyme responsive degradable carrier. Degradation was observed in the presence of the enzyme papain, which was chosen as model for the lysosomal cathepsin B.[76]

Polyacetals are more unstable under acidic conditions and are therefore prone to surface erosion.[77] One of the most famous example of polyacetal is Delrin® (polyoxymethylene), which found application in hearts implants in the 60s. Due to its degradation product formaldehyde, however, the employment for biomedical application was revoked. On the contrary, polyacetals based on the copolymerization of divinyl ethers and diols are much more biocompatible, degrade in non-acidic products, and exhibit temperature responsive features, rendering them candidate for biomedical application, such as drug delivery.[78]

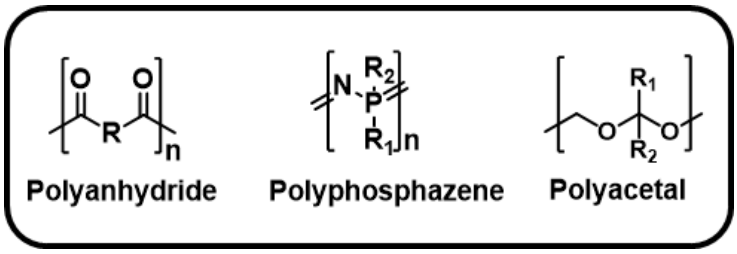

Figure 5. Structure of polyanhydrides, polyphosphazenes, and polyacetals. Depending on the nature of the "R," the anhydride can be aliphatic, unsaturated or aromatic. In polyphosphazenes, the "R" substituents are usually organic; the substituents can either be the same or different. Polyoxymethylene presents two hydrogens as R substituents.

1.2 The treatment of inflammatory diseases

1.2.1 Inflammation and activation of the complement system

In A.D. 25 Aulus Cornelius Celsus composed a work of 8 books, which is known as “De Medicina” and represents one of the first pieces on medicine. In this, it is already possible to find those which are recognized as the cardinal sign of an inflammation: rubor (redness), calor (heating), tumor (swelling), and dolor (pain).

Nowadays it is understood that inflammations are beneficial mechanisms that take place when a harmful situation is recognized and serve to restore the natural condition.[79]

The cells responsible for the removal of harmful agents are the leukocytes, also known as white blood cells. During the inflammatory process, the leukocytes are recruited from the blood vessel to the site of action and will accumulate there, originating the cardinal signs previously mentioned.[80] The redness is due to the increased blood flow, which as the same time comports the warming; the swelling results from the increased vascular permeability, as plasma fluids accumulate at the site of inflammation. Moreover, due to the release of pain transmitters, ache will be associated to the process.[81] To the previous mentioned marks, another cardinal sign was reported by Virchow in 1850: the “functio laesa” or loss of function, which can have different causes.[82]

Once the stimulus has been recognized, the recruitment of leukocytes proceeds in a cascade-like fashion. The steps are recruitment, tethering, rolling, slowing and arresting, and finally extravasation in the inflamed tissue (Figure 6).[83]

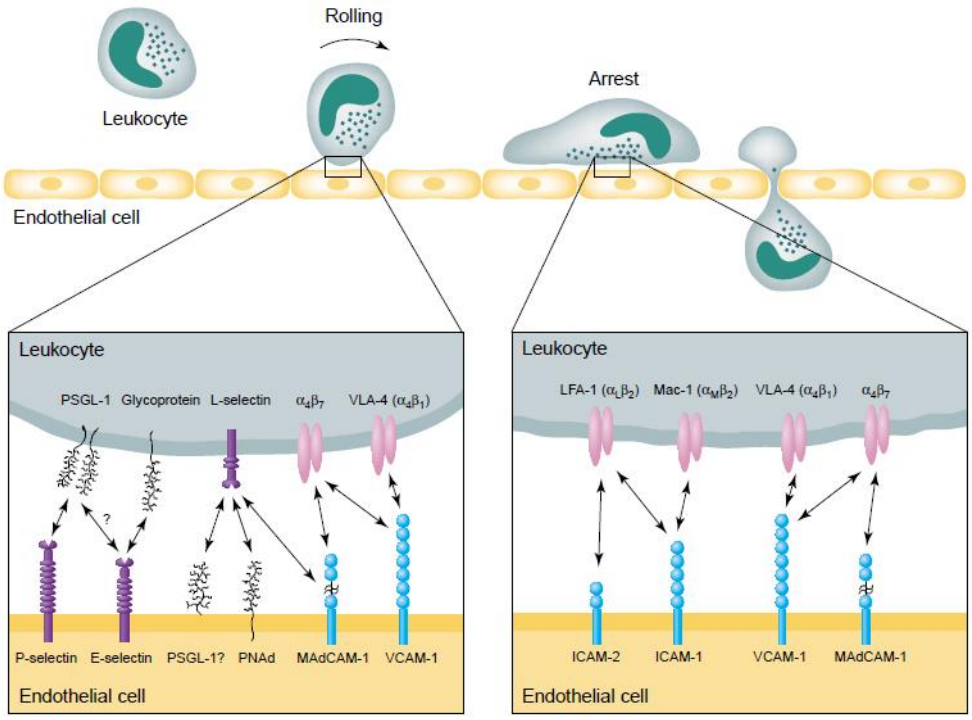

Figure 6. Illustration of the mechanism of leukocytes extravasation in the inflamed tissue. Adapted with permission from Ulbrich et al.[84] (Copyright 2014, Elsevier Inc.).

A fundamental aspect to initiate the recruitment is the production of chemicals signals such as pro-inflammatory cytokines, like tumor necrosis factor alpha (TNF-α) and interleukin-1 (IL-1), which are released by macrophages, dendritic cells and mast cells.[85] The binding of TNF-α and IL-1 to their receptors activates the cell adhesion molecules (CAMs), which mediate the interaction of leukocytes with the endothelium. CAMs can be divided into three major families: (i) the selectins, (ii) the integrins, and (iii) adhesion molecules, which belong to the immunoglobin (Ig) superfamily.

The selectins play a pivotal role in the mediation of tethering and rolling on the endothelium. These receptor-mediated interactions enable to slow down the passing of leukocytes.[86,87]

Selectins are glycoproteins and depending on the site of expression they can mainly be divided in three categories. P- and E- selectins are expressed on platelets and vascular endothelium, while L-selectins are expressed on leukocytes. Diverse studies have demonstrated the fundamental role of selectins for the leukocyte recruitment and extravasation. For example, this has been proven in knock-out mice lacking selectins, where delayed leukocyte extravasation was observed.[88,89]

In addition, the activation of integrins on the surface of leukocytes is necessary to induce the slowing of the leukocyte and intercellular adhesion molecules (ICAMs), vascular adhesion molecules (VCAMs) and junction adhesion molecules (JCAMs) are responsible for the formation of

firmly adhesive interactions. Finally, the transmigration from the blood vessel to the inflamed tissue takes place, being also facilitated by the matrix metalloproteinases (MMPs).

Another key player during an inflammation is the complement system. It is composed of proteins secreted mainly by the liver and membrane proteins, which collaborate to the opsonization of pathogens. There are three distinct pathways through which the complement can be activated: (i) the classical (CP), (ii) the lectin (LP), and (iii) the alternative pathway (AP). The only pathway, which is always active also in healthy people, at a low level, is the AP, while a complete activation of the complement is present only in case of infections. The activation on the cell surface favors the elimination of apoptotic cells, without releasing danger signals.[90]

The activation of all the three pathways comports the activation of C3 protein, which is the central component of the complement system. This is converted to C3a and C3b, which further induce activation events. C3a is a promotor of the inflammation, while C3b is an opsonin. As a result of the C3 activation, the C5 protein is activated and converted to C5a and C5b. Of these, C5b can bind to other proteins of the complement such as C6, C7, and C8 and form a membrane-attack complex (MAC) that is able to intercalate the membrane of some bacteria and to provoke their death. C5a is an anaphylatoxin as C3a and contributes therefore to the control of the inflammation (Figure 7).

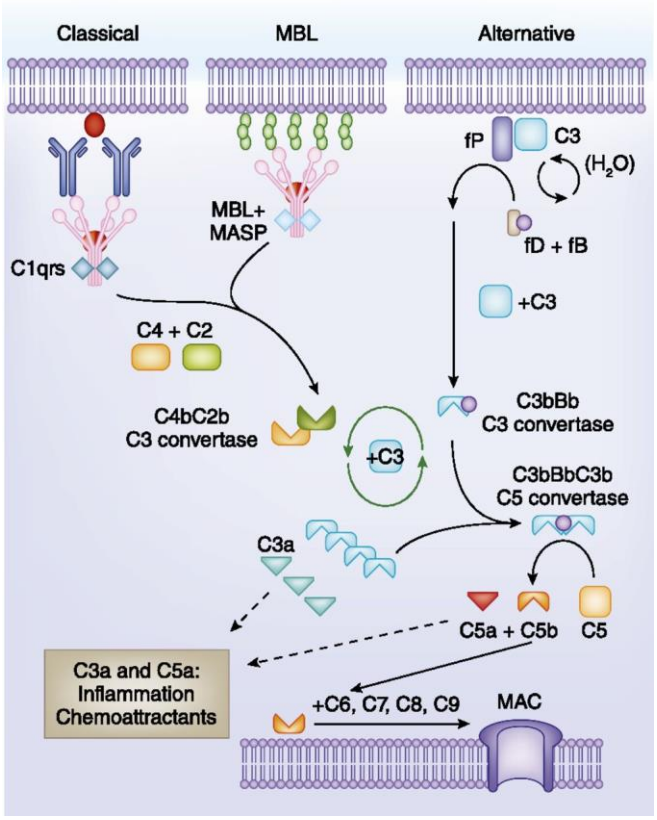

Figure 7. Schematic representation of the complement cascade. Reprinted with permission from Mathern and Heeger[91] (Copyright 2015, American Society of Nephrology).

1.2.2 The selectins and targeting of inflammation

As previously explained, the inflammatory process is beneficial and usually results in an acute event that rapidly restores the natural healthy environment. However, in case of chronic inflammations, the whole course is upregulated and instead of being helpful it can lead to tissue damaging. For this reason, a lot of effort has been spent to develop inhibitors of CAMs, in particular in relation to their activation operated by TNF-α,[92,93] which could be used for short-term therapies. Moreover, the targeting of selectins appears to be a promising approach for the control of leukocyte recruitment.

All the three selectins possess similar extracellular domains (Figure 8). They present carbohydrate binding, they have lectin domains that are calcium dependent (Ca^{2+}, C-type) and N-terminal, and they possess an epidermal growth factor domain (EGF), some consensus repeats, a transmembrane domain, and a cytoplasmic domain.[94] Of these domains, the lectin and EGF ones have been recognized to be fundamental for the specific binding of selectins to their ligands.

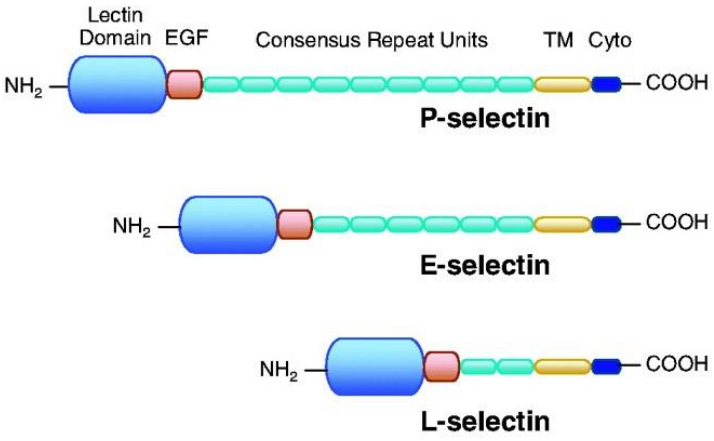

Figure 8. Schematic representation of the selectins. The domains, which characterize all selectins, are highlighted. Selectins differ in the number of short consensus repeats (2, 6, and 9 for L-, E,- and P-selectin, respectively). Adapted with permission from Hanley et al.[95] (Copyright 2004, Company of Biologists LTD.)

In particular, the selectins display a high affinity for ligands containing carbohydrate motifs like sialyl Lewis x (sLe^x) or sialyl Lewis A (sLe^a), which are present at the N- and O-terminus of some glycans. The recognition of these sugars is considered to be accountable for the adhesion of leukocytes to the endothelium. The epitope (NeuNAcα2-3Galβ1-4[Fucα1-3]GlcNAcβ1-R) displayed by sLe^x was found to be the common recognition determinant for all three selectins (Figure 9). [96]

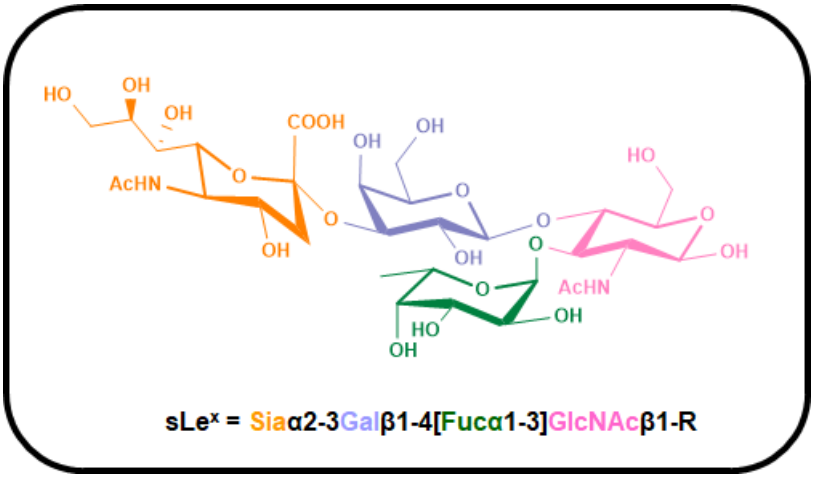

Figure 9. Structure of the binding motif of sialyl Lewis x (sLe^x).

The most important, abundant, and well-characterized ligand for selectins is represented by the P-selectin glycoprotein ligand-1 (PSGL-1).[96,97] This unspecific ligand is present as a homodimer on the leukocytes and on the activated endothelium and can bind to all the three

selectins. Similar to sLe^x and to sLe^a, PSGL-1 presents O- and N-linked carbohydrates and is stabilized via disulfide bridges. Moreover, it presents sulfated tyrosine residues that enhance its interaction with selectins. The binding to sulfated tyrosine residues has also been considered fundamental for P- and L-selectin, while sulfation does not seem to affect or enhance the binding to E-selectin.[98] The binding of selectins to PSGL-1 is so important, because it exhibits K_D values (dissociation constant values) in the μM range, while for sLe^X only mM binding can be reached. The development of synthetic oligosaccharides based on sLe^X has highlighted that the reproduction of the *in vivo* scenario and the strong binding is highly problematic. It can be reproduced only when sugar moieties are presented in a multivalent way.[99] The concept of multivalency is a key notion of biological systems, and is employed to magnify weak reversible interactions.[100] In particular, multiple ligands of one system cooperate to bind multiple receptors of the counterpart.

1.2.3 Polyanions for the treatment of inflammatory diseases

The peculiar role of selectins in the inflammatory states has rendered them a target in the therapy for overexpressed immune responses.

The approaches can mainly be divided in two families: (i) blocking the interaction of the selectins with their ligands or (ii) blocking the enzymes which are responsible for the variation of the ligands. Even though both approaches are promising, the development of ligand mimetics is predominant [101]

Diverse sulfated sugars have been investigated as potential selectins' inhibitors, among them heparin. Heparin is a highly sulfated glycosaminoglycan (GAG) widely used in the medical field as anticoagulant. It is usually obtained as a mixture of diverse molecular weights, known as unfractionated heparin (UFH), and due to its mammalian source, the transmission of illness might take place. Moreover, due to its highly anticoagulant and antithrombic effect, the use of heparin must be restricted, to avoid uncontrolled bleeding. Heparan sulfate is also an anionic sugar, which has the same repeating unit of heparin but a lower level of sulfation; it is usually present in the extracellular matrix (ECM) and shares the mammalian origin with heparin. Moreover, both heparin and heparan sulfate present the specific binding site of antithrombin III (AT), which is required to perform the anti-coagulant activity.[102] (Figure 10)

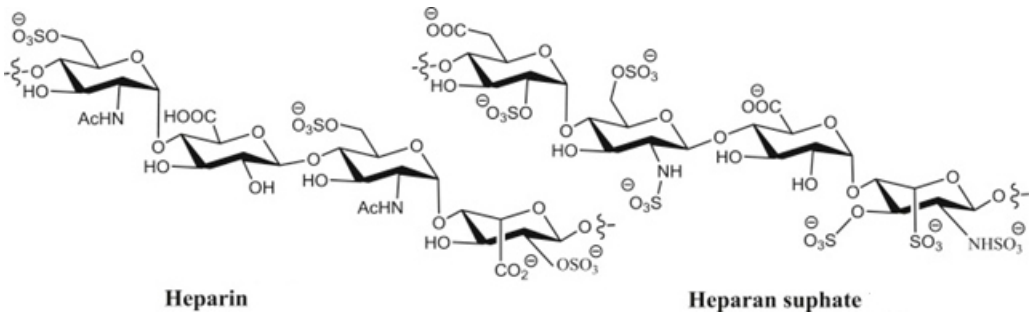

Figure 10. Structural comparison of heparin and heparan sulfate. The structures mainly differ by the hydroxyl groups that can be O-sulfonated and the amine can be N-acetylated, N-sulfated, or non-substituted. Adapted with permission from Mishra et al.[103] (Copyright 2016, Elsevier B.V.)

To overcome the major drawbacks of heparin, synthetic compounds such as fucoidan, synthetic polysulfates and other heparin derivatives have been taken into account. The polysaccharide fucoidan was demonstrated to be a suitable analog of heparin, as *in vivo* studies reported the inhibition of thrombus formation in mice.[104] In 2001 the methyl glycoside analog of the anti-thrombin pentasaccharide sequence of heparin was approved, and Fondaparinux (Arixtra™) found employment in the prevention of venous thromboembolism. The product is highly selective for the anticoagulation factor Xa.[105]

In 2004 a synthetic dendritic polyglycerol sulfate (dPGS) was presented by Türk et al. as heparin analog.[106] This polymer demonstrated not only to present a lowered anticoagulant activity but also other favorable characteristics of heparin, such as an enhanced anti-complement activity. dPGS is the sulfated derivate of the previously presented dendritic polyglycerol (Chapter 1.1.2). It is obtained via the conversion of the terminal hydroxyl groups to sulfates.

Due to the biocompatibility of polyglycerol and the rich composition in functionable end groups, Haag and coworkers prepared a polyvalent sugar-based selectin inhibitor. While the hPG itself exhibited no binding, the multivalent galactose-terminated architectures showed inhibition in the nM range, especially after sulfation. [107]

The estimation of the potential as inhibitors is given using an *in vitro* assay developed by Enders and coworkers.[108] In a surface plasmon resonance (SPR) setting, a competitive binding test is conducted. Gold nanoparticles (Au NPs) are coated with selectins in order to mimic the leukocytes, and passed over a chip, which is itself coated with the ligand motifs of selectins (sialyl Lewis x, tyrosin sulfate) to mimic the endothelium (Figure 11). The binding of the Au-NPs to the sensor chip is defined as the maximal possible and set as 100%. Afterwards, Au-NPs previously incubated with the potential inhibitor are also passed over a chip mimicking the endothelium and the reduced binding signal is registered in a concentration dependent way. The concentration of

inhibitor necessary to reduce the binding of the 50% is defined as the IC_{50}. The lower the concentration of the IC_{50}, the better potential as inhibitor is assigned.

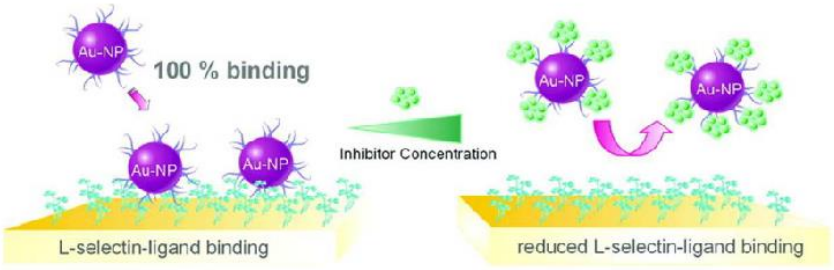

Figure 11. Schematic representation of the SPR assay for the determination of the inhibitory capacity of synthetic selectin ligands. Adapted with permission from Weinhart et al.[109] (Copyright 2011, American Chemical Society).

In 2010 Dernedde et al. demonstrated the capability of dPGS as macromolecular inhibitor for the binding of selectins to their ligands on the endothelium. The reduction of P- and L-selectin adhesion was investigated via the SPR assay previously described. Moreover, the reduction of the activation of the complement factors C3 and C5 was also observed.[110]

Further studies from the Haag group focused on the development of diverse anionic functionalized dPG and their application as L-selectin inhibitors.[109] dPGS was compared with the corresponding carboxylate (dPGC), sulfonate (dPGSn), phosphonate (dPGPn), bisphosphonate (dPGBP), and phosphate (dPGP). It was observed that, even though all the functionalities had an influence on the binding of selectins, no other derivative was able to compete with the outperforming dPGS. Moreover, it was detected that the inhibitory potential was related to the degree of sulfation of the dPGS. Furthermore, the role of size and charge was investigated, and it was possible to recognize that, besides the electrostatically interactions of the dPGS with the positively charged selectins, the spatial arrangement played a role on the force of the interaction. [111] As a further confirmation, the role of the branching on the inflammation was investigated and it was showed that an optimal performance was based on the branching and the flexibility of the polymer.[112]

For the application as delivery system *in vivo*, the possibility of accumulation in the organs has to be taken into account. For this reason, radio-labelled dPG and dPGS were synthesized and their pharmacokinetics were evaluated.[113] As accumulation of dPGS was mainly observed in the spleen and the liver, the necessity of the development of biodegradable dPGS arose. Recently, cleavable linkers were introduced between the core and the shell of the dPGS to obtain a biodegradable

system.[114] These polymers exhibit a strong inhibitor capability in the nano/picomolar range and can be hydrolytically or enzymatically degraded to the more compatible dPG.

1.3 Nanocarriers for the delivery of chemotherapeutics

1.3.1 Introduction to cancer therapy

One of the principal causes of death worldwide is represented by cancer, with a generally growing incidence. The most diagnosticated form of cancer and at the same time the first one for mortality is lung cancer, followed by breast and colorectal cancer.[115,116]

The common treatments are chemotherapy (the treatment of cancer with drugs), surgical removal and radiation (external or internal treatment with ray to destroy the tumor).
Examples of commonly used small molecule drugs in chemotherapy are doxorubicin, paclitaxel, vincristine and cisplatin (Figure 12).

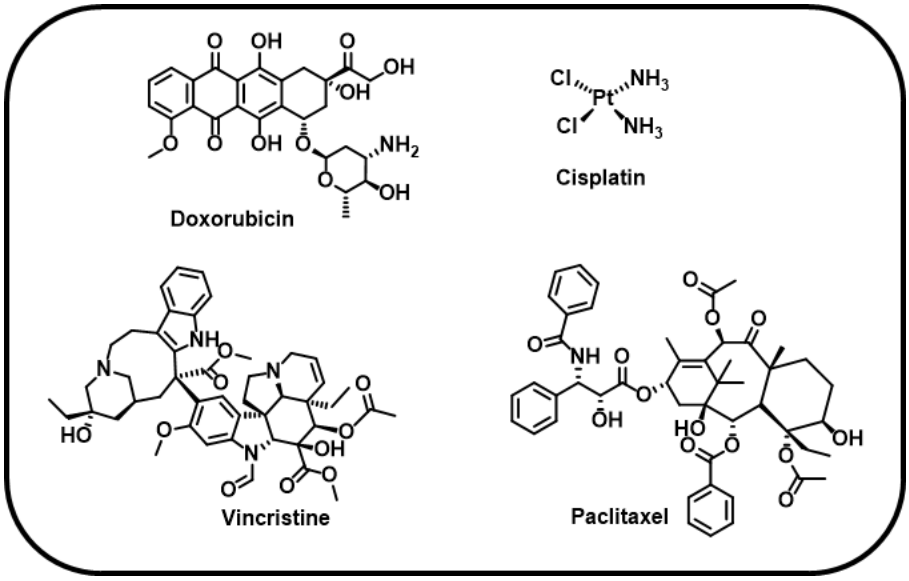

Figure 12. Examples of drugs commonly used for the treatment of cancer.

Doxorubicin is a cytostatic drug, due to its ability to intercalate into DNA; paclitaxel and vincristine act by inhibiting the mitosis. Cisplatin is an alkylating agent and exploits its activity by directly binding the DNA and inhibiting its division. Even though all these drugs are highly potent, the lack in selectivity toward tumor cells entails diverse side effects, leading therefore to the need of carriers for their delivery. Some of them have already been approved by the FDA and have entered the market, such as Doxil® (Pegylated liposomes loaded with doxorubicin) or Abraxane® (an albumin-based formulation of paclitaxel).[117]

For further improvement of the cancer therapies, a profound understanding of the mechanisms, which regulates the tumor development and growth, is necessary. For this purpose, Weinberg and Hanahan have compiled a list of six hallmarks, which seem to be shared by almost all

cancer types (Figure 13). Cancer tissue is characterized by the independence from normal growth factors, as the cells are able to produce their own growth signals, while escaping the growth suppressor. Moreover, the cancer cells can assault and invade the neighbor tissue, resulting in an uncontrolled proliferation. Additionally, cancer is able to induce the formation of new blood vessels, which supply it with the necessary nutrients, and has develop mechanisms which prevent the normal clearance of damaged cells (apoptosis).[118]

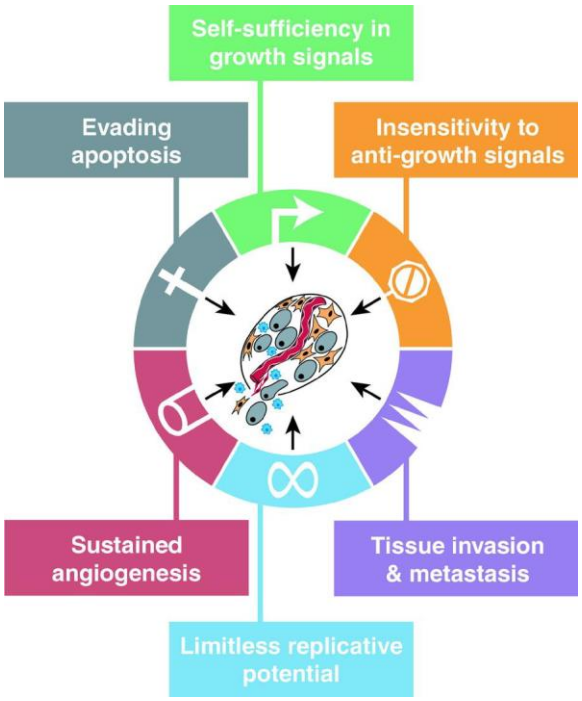

Figure 13. The hallmarks of cancer described by Weinberg and Hanahan. Reprinted with permission from Weinberg and Hanahan[118] (Copyright 2000, Cell Press).

Besides the aptitude of being extremely proliferative and resistant, numerous cancer types seem also to be able to reprogram the cell metabolism to ensure the continuous growth, and moreover to be able to escape the action of immune cells.[119,120] The local acidic pH exhibited by tumors has been attested to the shift from energy metabolism to glycolysis. In absence of oxygen, pyruvate is converted to lactate by lactate dehydrogenase (LHD), whose accumulation leads to the decrease in pH. This alteration is known as the "Warburg effect". Interestingly, the glycolysis in tumor can happen even under anaerobic conditions.[121] Another key factor for the cancer immune escape can be attributed to hypoxia. The low perfusion of oxygen and the chemicals reactions, which happen in the cancerous site, induce the local acidic pH. This renders the environment unfriendly to immune cells, which are therefore disarmed in their activity. [122] Moreover, there is increasing evidence that the level of reactive oxygen species (ROS) in the tumor environment is

higher than in the normal tissue, which provokes an enhanced oxidative stress. Since the role of the ROS production is, however, still unclear, the possibility of treating cancer by controlling the ROS imbalance is under investigation.[123] Finally, there is a growing investigation of the role of immune response in the development of cancer, as chronic inflammations and tumor are known to be related events.[124] The expression of E-selectin has, for example, been found to be associated to angiogenesis and metastasis of diverse cancers.[125]

All these factors contribute to reduce the efficiency of cancer treatments, and induce low specificity, limited uptake, and rapid degradation of drugs. Nanomedicine represents, however, a suitable tool to develop carriers capable of escaping the natural clearance mechanism and use the unique traits of cancer to fight it in a much more precise manner.

1.3.2 The delivery of chemotherapeutics: active and passive targeting

A suitable strategy for the treatment of cancer is to use nanocarriers, which can implement the targeting and drug release at the site of action. This purpose can be mainly achieved via two approaches: the active and passive targeting.[126,127]

Active targeting is exemplified by the previously reported Ringsdorf model (Chapter 1.1.1). Besides the drug, specific ligands can be attached to the polymeric backbone, which ensure the interaction only with defined receptors. To this purpose, the receptors that are overexpressed at the site of accumulation are usually addressed. Diverse molecules can be used as ligand, ranging from anti-bodies to proteins, from peptide to nucleic acids.[128]

Folic acid, a member of the vitamin B family, finds, for example, employment in the targeting of rheumatoid arthritis, as an over-expression of its receptors on macrophages is usually associated with the disease.[129,130] Recently Wang et al. reported the synthesis of doxorubicin loaded, lipid-based nanoparticles presenting double ligands, namely the peptide ANG2 and aptamer AS1411, for the enhanced penetration of the blood–brain barrier (BBB) and the treatment of gliomas.[131]

The design and development are, however, complicated due to the chemistry beyond these architectures and the problems related with the administration *in vivo*, which can reduce the effectiveness.

The passive targeting is an approach, which finds mostly employment for targeting tumoral tissue, as the enhanced permeation and retention (EPR) effect will be displayed. This effect was described by Maeda et al. in 1986.[132,133] The cells of the endothelium grow in a tightly compact form, while in the case of tumor or inflammation, the cells growth is uncontrolled and irregular, leading to a porous and disrupted tissue. Whereas small molecules would enter both healthy and

diseased tissue, undergoing rapid clearance through the lymphatic system, macromolecules are able to enter only the irregular tumor tissue. Moreover, due to the reduced lymphatic drainage, they will be preferentially accumulated there (Figure 14).

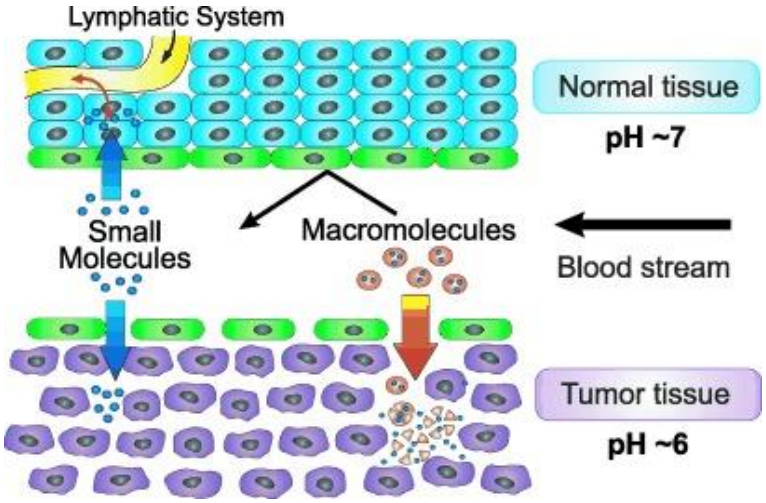

Figure 14. Schematic comparison of healthy and cancer-affected tissues. Due to the enhanced permeability, macromolecules can penetrate and accumulate in the tumor tissue (EPR effect). Reprinted with permission from Haag and Kratz[134] (Copyright WILEY-VCH Verlag GmbH & Co. KGaA, Weinheim).

The EPR effect can be exploited by diverse compounds, such as proteins, peptides, synthetic nanoparticles, and DNA.[135] However, major concerns about the effectiveness of this effect in patients, due to the extreme diversity of the tumoral tissue, have led to the investigation of systems, which can also sense other typical features of cancer.

1.3.3 Stimuli responsive nanocarriers and the delivery of anticancer drugs

The release of a drug at a specific site of action is obtained by designing stimuli-responsive DDS. The carrier responds to a specific cellular, chemical, or physical stimuli, which provoke a change in the structure of the carrier and therefore the release of the cargo is promoted. This mechanism is presented in Figure 15.

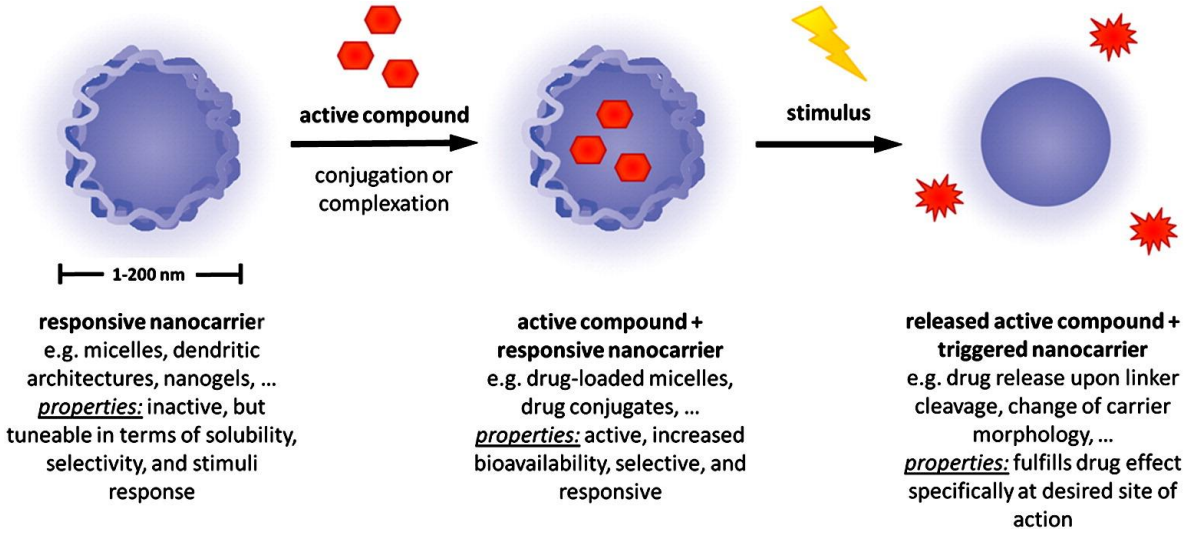

Figure 15. Mode of action of trigger release under defined stimuli. Reprinted with permission from Fleige et al.[136] (Copyright 2012, Elsevier B.V.).

There are diverse triggers employed to induce the drug release, which can mainly be divided in endogenous and exogenous. Exogenous stimuli are light, magnetic field, ultrasound, and temperature, while endogenous stimuli are pH, enzymes, ionic strength, and redox potential.[137]

The loading of guest molecules is usually obtained through two approaches: (i) the guest is physically entrapped within the carrier and (ii) the active compound is covalently attached to the scaffold of the macromolecule, either on its backbone or on the terminal groups. Depending on the loading strategy and the type of stimuli, the release can be achieved in different ways. In the first case, the release of the drug is obtained via disruption or conformational changes of the carrier, as the guest is entrapped in the interior of the carrier, while in the case of covalently attached drugs only the link between the carrier and the active compound should be cleaved.

In the following, the three most significant stimuli present in tumor tissue and the related type of release will be presented.

pH triggered release

It is generally known that the human body depicts a neutral pH, with the exception of specific compartments which have to carry out distinct actions. This is the case of the stomach, which necessitate acidic pH to degrade the food, or of the intestine, which exhibit a more alkaline pH up to 8 in the colon. The pH, however, decreases also in case of pathological conditions as an effect of the abnormal metabolism. As a result, inflamed and tumoral tissues are generally characterized by an acidic pH of the extracellular milieu. Moreover, the drop of the pH is a typical aspect also in the cellular compartment: even though early endosomes exhibit an almost neutral pH (6-7), in the late

endosomes and lysosomes a drop to 4-5 is reported.[138] As basic pH is usually not exhibited in case of illness, the stimuli responsive carriers are mainly developed to respond to acidic conditions.

In order to obtain a pH responsiveness, hydrolytically cleavable moieties can be employed. The cleavable linkers reported in Figure 16 undergo hydrolytic cleavage in the pH range 4-8.[136]

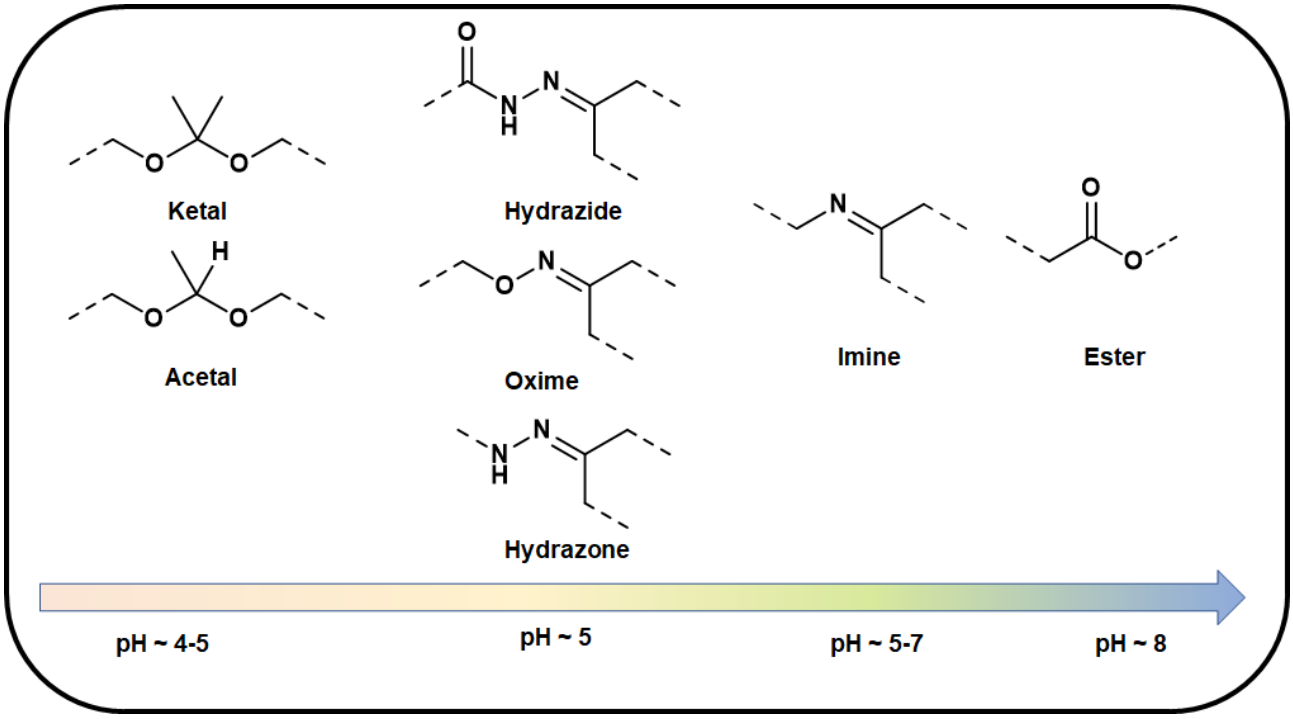

Figure 16. Examples of pH responsive functional linkers. The pH at which the bond should break is reported.

Core-shell architectures of magnetite (Fe_3O_4) and silica (SiO_2) were used as core for the development of triazine dendrons and loaded with methotrexate (MTX). These structures exhibited high loading capacity and fused the strategy of magnetic targeting with the release upon a pH drop to 5.5.[139] Recently, polysaccharides were screened for the preparation of pH-sensitive doxorubicin-conjugates containing imine bonds. Dextrane, which emerged as the best candidate, showed a marked pH-dependent release rate, concerning the *in vitro* release in the pH range from 7.4 to 5. Moreover, *in vivo* tests confirmed the antitumor ability and displayed limited adverse effects in comparison with free doxorubicin.[140]

The necessity to exploit diverse features using only one carrier has also led to the development of theranostics, in which the therapeutic effect and the diagnostic tools, such imaging agents, are combined.[141] The group of Wu developed pH sensitive micelles and vesicles for imaging and drug delivery applications. Upon the self-assembly in micelles and vesicles, fluorescence was exhibited due to the presence of aggregation-induced emission (AIE) luminogens.

Doxorubicin release under acidic conditions was observed, and the drug distribution could be followed taking advantage of the fluorescence resonance energy transfer (FRET) between doxorubicin and the tetraphenylethylene (TPE) present in the polymer chain.[142]

Calderon et al. have used hPG for the development of pH responsive drug-conjugates, in which doxorubicin was attached to the polymer using hydrazone as the cleavable linker. Moreover, a PEG shell was attached to prevent the preventive clearance and tumor growth inhibition could be observed in an ovarian xenograft tumor model.[143]

The dendritic polyglycerol sulfate (dPGS) has been demonstrated to be not only an appropriate polymer for the treatment of inflammatory states (Chapter 1.2.3) but also to be a suitable building block for nanocarriers in the delivery of anticancer drugs. A dPGS-paclitaxel conjugate (dPGS-PXT) was prepared by the introduction of an ester bond between the drug and the polymer, which could be internalized by cells but displayed poor stability and premature drug release.[144]

Enzymatic triggered release

As previously mentioned in the chapter about biodegradable polymers (Chapter 1.1.3), enzymes can degrade nanocarriers depending on the presence of specific bonds. In the same way, nanocarriers that respond to the presence of definite enzymes can be designed. In the case of the treatment of cancer, some enzymes are recognized to be overexpressed in the tissue and can therefore be used as target or trigger. Examples of these are proteases, glucuronidases and carboxylesterases.[145]

Zhao and coworkers reported on an amphiphilic peptide that disassembled in response to fibroblast activation protein-a (FAP-a), which is overexpressed by a cancer-associated fibroblast. The complete release of the doxorubicin loaded in the carrier was obtained within 3 hours, when the system was treated with FAP-a, while the untreated compound showed only a moderate release within 48 hours. Moreover, cytotoxicity tests confirmed the specificity of the carrier to FAP-a, as no significant toxicity was detected with the tested cell lines.[146]

Haag and coworkers have reported the synthesis of hPG based prodrugs which can be cleaved by the action of cathepsin B. Both doxorubicin and methotrexate were conjugated with hPG and the activity of the prodrug was compared to that of the free drug. This approach was particularly successful for the prodrug made from methotrexate.[147]

Secreted phospholipase A2 (PLA2) is also a protein which is overexpressed by numerous tumors, including breast, pancreas, and colon, and has therefore been often chosen as a target.[148] Degradable liposomes, which have DNA nanoclews as the core, were loaded with tumor necrosis

factor-related apoptosis-inducing ligand (TRIAL), to obtain an anticancer activity via inhibition of the endocytosis.[149]

For the targeting of phospholipase C (PLC), which is implicated in the evolution of cancer cells, dendrimers containing phosphite ester bonds were recently synthesized and loaded with doxorubicin. The dendrimers exhibited a prolonged blood circulation when the surface was functionalized with zwitterionic groups and a greater therapeutic effect in comparison to the free drug.[150]

The extremely particular environment of cancer has also led to the development of nanocarriers that can respond to dual stimuli. Saxena and Jayakannan, for example, have synthesized polyester-based lysosome-responsive nanocarriers, which can release the cargo due to a drop of pH and then can be degraded in the presence of an esterase, which mimic a lysosomal enzyme.[151]

Redox triggered release

Diverse redox couples are present in the human body, of which glutathione (GSH) GSSG/2GSH is one of the most interesting, as it represents one of the major redox buffers.[152] Higher glutathione concentration can be observed in the cytoplasm and cancer cells and have been widely investigated as a trigger for the rupture of disulfide bonds.[153,154]

The incorporation of a polypeptide in the copolymer poly(ethylene glycol)-*block*-poly-L-phenylalanine (mPEG-SS-PPhe) via a disulfide linker has led to the synthesis of redox-responsive micelles for the delivering of doxorubicin. These have been shown to be stable in the physiological environment and to dissociate in the presence of 10 mM GHS, also releasing their cargo in a GHS concentration dependent way.[155]

Micelles based on poly(styrene-co-maleic anhydride) were functionalized with a peptide containing the arginylglycylaspartic acid (RGD) sequence to enhance the tumor targeting and crosslinked with cystamine, which represents the redox-sensitive moiety. This approach allows for the fabrications of nanocarriers which fuse the active targeting to the trigger release strategy.[156]

Zhong and coworkers have presented micelles of dPGS and polycaprolactone connected via disulfide likers, which exhibit extremely tumor targetability and *in vivo* chemotherapy (Figure 17).[157] Recently, Haag and coworkers conjugated monomethyl auristatin E (MMAE) with dPGS, obtaining a redox sensitive polymer-drug conjugate, which demonstrated improved cellular uptake and cytotoxicity *in vitro*, and avoid cytotoxic effects *in vivo*.[158]

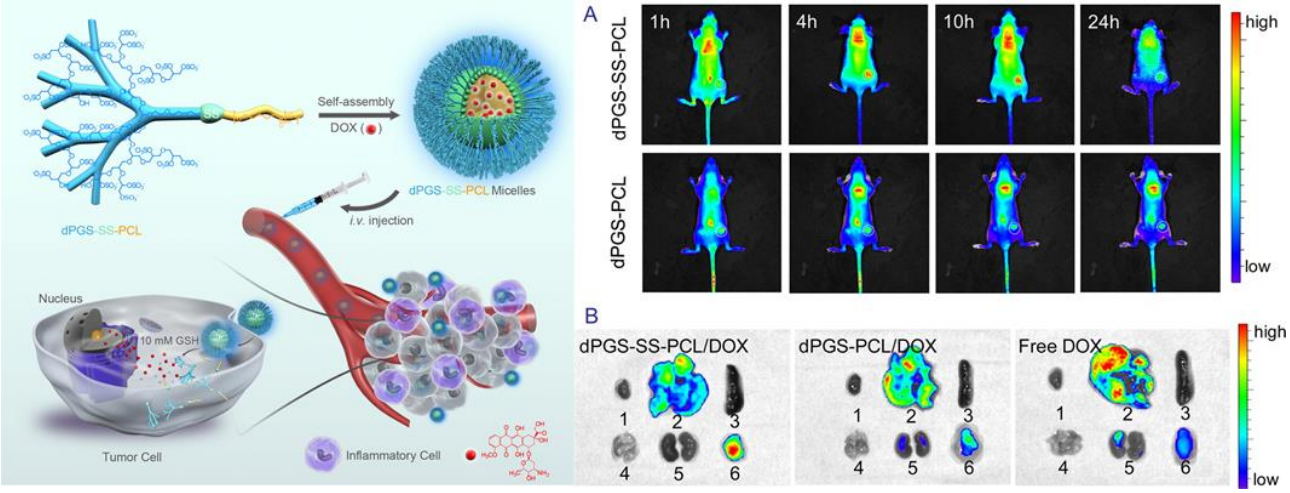

Figure 17. Example of the employment of dPGS for tumor targeting and treatment. dPGS based micelles present extremely high targetability *in vivo*. Adapted with permission from Zhong et al.[157] (Copyright 2016, American Chemical Society).

2 Objectives

The poor bioavailability of drugs when administered to the patients is a major concern in medicine. For the enhancement of drugs effectiveness and to reduce the undesired side effects, delivery systems have been studied and developed over the last five decades. Nowadays researchers are able to synthesize nanocarriers that can sense the environment and release the cargo at the desired site of action. Moreover, continuous improvement of the delivery systems has led to the production of polymeric materials with enhanced biocompatibility and biodegradability. The deepening of the knowledge of the pharmacokinetics and the processes that govern illnesses has also allowed the design of synthetic compounds which can exploit pharmaceutical activity themselves.

The aim of this doctoral work is the development of biodegradable polymers based on polyglycerol and their employment for biomedical applications. To reach this goal, a new biodegradable copolymer will be employed both as mediator of the inflammatory response and as nanocarrier for hydrophobic small molecules.

Sulfated biodegradable hyperbranched polymers based on polyglycerol and polycaprolactone are prepared and investigated for the inhibition of L-Selectin and the control of inflammatory processes. It has been demonstrated that dPGS is a suitable moiety for the inhibitions of L-selectin, but its lack of biodegradability restrains its usage. The new biodegradable copolymer (hPG-co-PCL)S shall be synthesized and tested as inhibitors of the L-selectin. Also, the induction of adverse effects such as toxicity or the affection of blood coagulation will be investigated. Screening *in vitro* will be conducted to confirm the biocompatibility of the copolymer and its influence on blood clotting, while a great inhibition potential with regard to L-selectin and the complement system is expected. The degradation of the compound in presence of enzymes should lead to the production of non-toxic species.

A nanocarrier should be able to enhance crucial aspects of the pharmacokinetics of drugs, such as their solubility, viability, uptake, and ideally target only the diseased tissue. Diverse designs can be employed to obtain such nanocarriers, mainly via covalent conjugation of the drug to the polymeric backbone or via physical entrapment in the carrier. In relation to this doctoral work, both the approaches are under investigation, to determine the versatility of the carrier in relation to diverse loading approaches. For the development of a drug-conjugate, the copolymer is employed as a macromolecular initiator for the polymerization of polycarbonates, which are afterwards functionalized with amines as terminal groups, to achieve both the conjugation and the physical interaction with the antitumoral drug gemcitabine. The new systems should be biocompatible prior the loading of the antitumoral compound, while being able to release the guest under pH drop, a

typical feature of cancer. The activity and stability are screened *in vitro* to confirm the eligibility as nanocarrier.

For the translation of the research from the laboratory level to the industry one, synthetic approaches with high manufacturing volume and low production costs are required. In this thesis, the possibility to optimize the synthesis of the biodegradable nanocarrier to implement the control over the molecular weights and augment the gram scale production will be investigated. Moreover, the use of the copolymer, prior and after sulfation, as a carrier for diverse hydrophobic compounds will be taken in account. The employability as nanocarriers will be tested using diverse hydrophobic molecules, namely, doxorubicin and a near infrared dye. The design of a sulfated copolymer is chosen not only to obtain an anti-inflammatory potential but also to target the tumor environment. The *in vitro* screening of the guest molecules shall demonstrate which interactions are favored, and which carrier is the best performer. I*n vivo* test will be conducted to confirm the ability of the carrier in targeting the cancer and the suitability of the copolymer for further *in vivo* studies. The objectives of this thesis are schematically depicted in Figure 18.

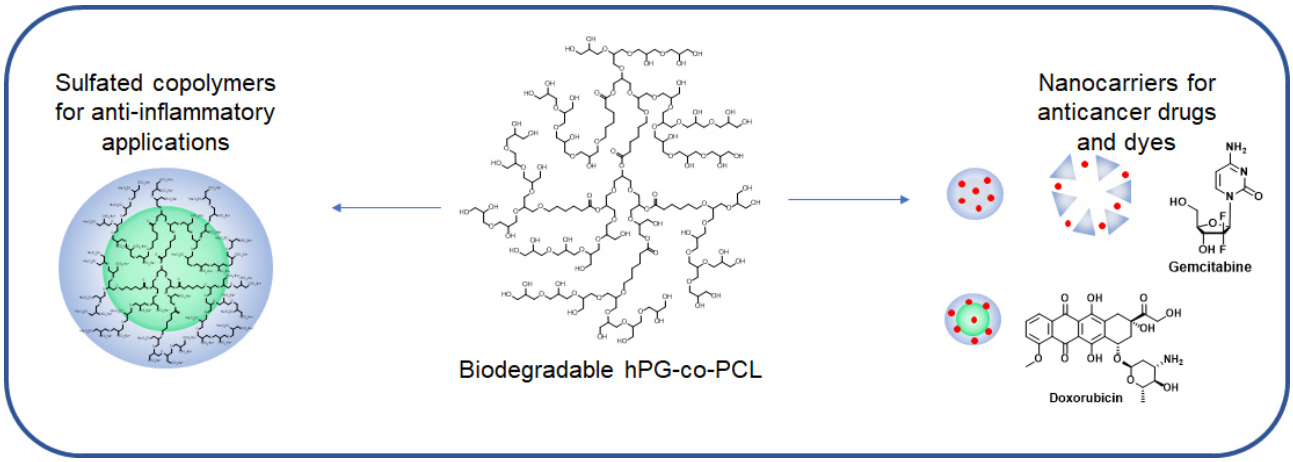

Figure 18. The biodegradable hPG-co-PCL and its application in this thesis.

3 Publications and Manuscript

3.1 Biodegradable Polyglycerol Sulfates Exhibit Promising Features for Anti-inflammatory Applications

Magda Ferraro,[a] Kim Silberreis,[a] Ehsan Mohammadifar, Falko Neumann, Jens Dernedde, and Rainer Haag, *Biomacromolecules,* **2018***, 19(12),* 4524–4533.

[a] Equal contribution of the authors

https://doi.org/10.1021/acs.biomac.8b01100

Inflammatory processes are beneficial responses to overcome injury or illness. Knowledge of the underlying mechanisms allows for a specific treatment. Thus, synthetic systems can be generated for a targeted interaction. In this context, dendritic polyglycerol sulfates (dPGS) have been investigated as anti-inflammatory compounds. Biodegradable systems are required to prevent compound accumulation in the body. Here we present biodegradable analogs of dPGS based on hyperbranched poly(glycidol-co-caprolactone) bearing a hydrophilic sulfate outer shell (hPG-co-PCLS). The copolymers were investigated regarding their physical and chemical properties. The cytocompatibility was confirmed using A549, Caco-2, and HaCaT cells. Internalization of hPG-co-PCLS by A549 and Caco-2 cells was observed as well. Moreover, we demonstrated that hPG-co-PCLS acted as a competitive inhibitor of the leukocytic cell adhesion receptor L-selectin. Further, a reduction of complement activity was observed. These new biodegradable dPGS analogs are therefore attractive for therapeutic applications regarding inflammatory diseases.

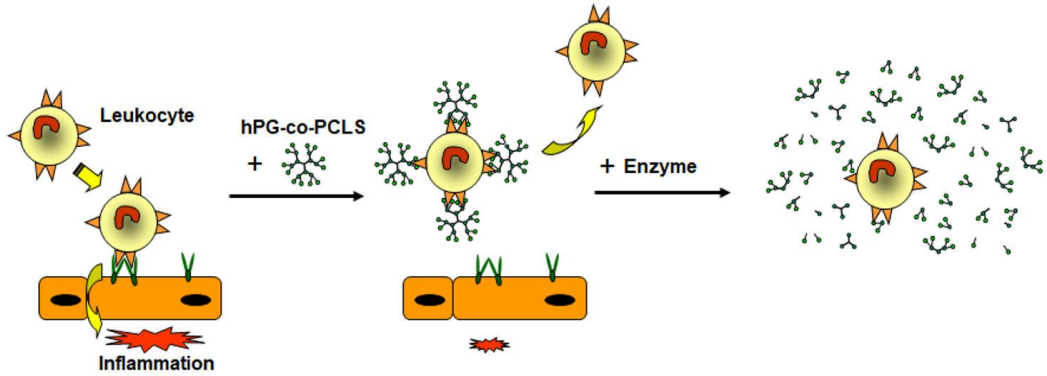

Contribution: Synthesis and characterization of the copolymers, viability tests, cellular uptake investigation, enzymatic degradation. Writing and editing of the document and figures, revision of the manuscript.

3.2 Dendritic Polyglycerol-derived Nano-architectures as Delivery Platforms of Gemcitabine for Pancreatic Cancer

Priyanka Ray, **Magda Ferraro**, Rainer Haag, Mohiuddin Quadir, *Macromolecular Bioscience,* **2019**, 19, 1900073

https://doi.org/10.1002/mabi.201900073

Dendritic polyglycerol-co-polycaprolactone (PG-co-PCL)-derived block copolymers are synthesized and explored as nanoscale drug delivery platforms for a chemotherapeutic agent, gemcitabine (GEM), which is the cornerstone of therapy for pancreatic ductal adenocarcinoma (PDAC). Current treatment strategies with GEM result in sub-optimal therapeutic outcome owing to microenvironmental resistance, and rapid metabolic degradation of GEM. To address these challenges, physico-chemical and cell-biological properties of both covalently conjugated, and non-covalently stabilized variants of GEM containing PG-co-PCL architectures have been evaluated. Self-assembly behavior, drug loading and release capacity, cytotoxicity and cellular uptake properties of these constructs in monolayer and in spheroid cultures of PDAC cells are investigated. To realize the covalently conjugated carrier systems, GEM, in conjunction with a tertiary amine, is attached to the polycarbonate (PC) block grafted from the PG-co-PCL core. It is observed that, pH-dependent ionization properties of these amine side-chains directed the formation of self-assembly of block copolymers in the form of nanoparticles. For non-covalent encapsulation, a facile 'solvent-shifting' technique has been adopted. Fabrication techniques have been found to control colloidal and cellular properties of GEM-loaded nanoconstructs. We report the feasibility and potential of these newly developed architectures for designing carrier systems for GEM to achieve augmented prognosis for pancreatic cancer.

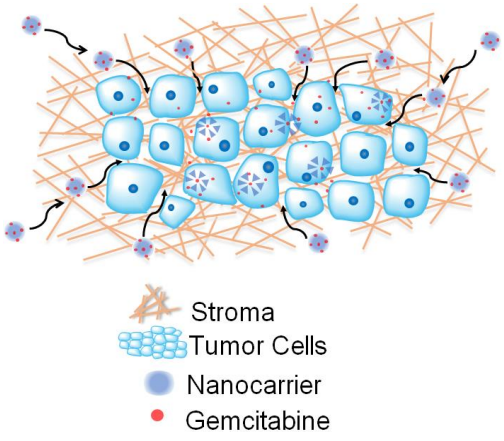

Contribution: Synthesis, chemical and physical characterization of the core copolymer PG-co-PCL. Writing and editing of the document and figures, revision of the manuscript.

3.3 Biodegradable Polyglycerol-based Copolymers for the Delivery of Hydrophobic Drugs and Dyes

Magda Ferraro,[a] Ehsan Mohammadifar,[a] Elisa Quaas, Carsten Grötzinger, Michael Schirner, Rainer Haag

[a] Equal contribution of the authors

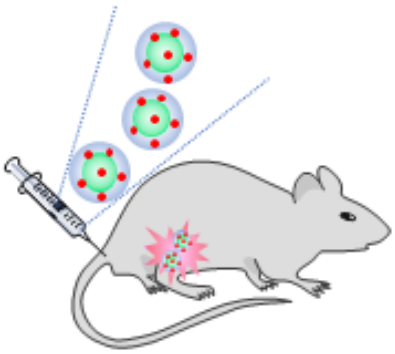

Contribution: Synthesis and characterization of the copolymers, prior and after sulfation. Loading tests with doxorubicin and NIR dye. Characterization of the loaded copolymers. Writing and editing of the document and figures, revision of the manuscript.

Biodegradable polyglycerol-based copolymers for the delivery of hydrophobic drugs and dyes

Magda Ferraro, Ehsan Mohammadifar, Elisa Quaas, Carsten Grötzinger, Michael Schirner, Rainer Haag

---

Magda Ferraro, Dr. Ehsan Mohammadifar, Elisa Quaas, Prof. Michael Schirner, Prof. Rainer Haag, Institute of Chemistry and Biochemistry, Freie Universität Berlin, Takustr. 3, 14195 Berlin, Germany

Prof. Carsten Grötzinger, Charite-Universitätsmedizin Berlin, corporate member of Freie Universität Berlin, Humboldt- Universität zu Berlin, and Berlin Institute of Health, Institute of Laboratory Medicine Clinical Chemistry and Pathobiochemistry, CVK Augustenburger Platz 1, 13353 Berlin, Germany
E-mail: rainer.haag@zedat.fu-berlin.de

Keywords: biodegradable, hyperbranched polymers, drug delivery, anticancer

Abstract

The low half-life of small molecules in the blood stream and the poor targeting of diseases are major concerns for their use in tumor therapy. To overcome this problem and enhance the efficiency of drugs, synthetic nanocarriers may be employed. Biodegradable and biocompatible polymers have already found extensive employment for drug delivery applications. This study aims to develop a simple and low-cost method to synthesize a biodegradable hyperbranched poly(glycidol-co-caprolactone) (hPG-co-PCL) by slow monomer addition and describes its use as nanocarrier for small hydrophobic compounds. The investigation of the copolymer performance prior and after functionalization with sulfate groups shows that the sulfated copolymers exhibit a great capacity regarding the loading of the anticancer drug doxorubicin and its enhanced uptake into the tumoral cell line Hela. A very low toxicity of the copolymer and a remarkable performance as nanocarrier is displayed, especially for the delivery at low drug concentrations (< 1 μM). In addition, the encapsulation of a near infrared dye and *in-vivo* fluorescence imaging studies reveal the accumulation

of dye-encapsulated sulfated hPG-co-PCL in the tumor tissues. These initial findings show the potential of the new copolymer for the delivery of anticancer drugs within the tumor environment.

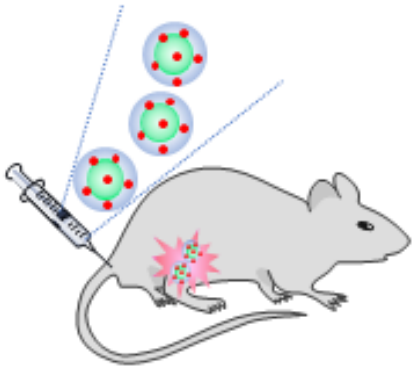

1. Introduction

A key role in the effectiveness of medical treatments is represented by the bioavailability of drugs, when administered to patients. Drugs are generally small molecular weight compounds, which easily undergo rapid renal clearance or non-specific distribute all over the body.[1] The low targeting capacity and overall distribution represent a relevant problem for the treatment of cancer.[2] Doxorubicin (Doxo) represents one of the drugs of choice in the treatment of various cancer types, both in children and adults.[3] This cytostatic compound acts by intercalating in the DNA and preventing its replication.[4] However, the compound is unable to distinguish healthy cells from cancer ones and therefore acts upon both. In addition, patients on Doxo-therapy often show a cardiac toxicity.[5]

To overcome this limitation and augment the effectiveness of drugs, nano-transporters can be employed. Nanocarriers are system with a defined size, generally between 10 and 100 nm, which help to improve the bioavailability of the drugs.[6] This strategy is particularly relevant for the enhancement of the delivery of chemotherapeutics. The employment of carriers enables in fact to provide a higher amount of drug to the desired site, while the delivery to the healthy tissue can be prevented.[7] Moreover, the nanocarriers can be constructed in order to respond to specific stimuli like change in the pH or in the redox potential, which are generally displayed by the tumor environment.[8] Furthermore, the nanocarriers can be functionalized with ligands like proteins or antibody to

specifically interact with receptors expressed by the tumor tissue.[9] Finally, due to the irregular growth of the tumor cells, which render the tissue permeable to big molecules, and the restrained lymphatic drainage, nanocarriers can preferentially accumulate in the tumor and release their cargo in this environment. This passive targeting is known as the enhanced permeation (EPR) effect.[10]

Dendritic polymers and liposome-based systems represent two suitable families for drug delivery. Liposomes find, in fact, already application in commercially available formulations, as for example Doxil (liposomal nanocarrier for doxorubicin),[11] while dendrimers and dendritic polymers offer favorable characteristics such as the potential of passive targeting by size.[12] In the past few years, different approaches based both on active and passive targeting, have been used to deliver doxorubicin and other anticancer drugs.[13,14]

Multilayer nanocarriers composed of a poly(amino amide) (PAMAM) dendrimer core, a hydrophobic layer of polycaprolactone (PCL) and an outer hydrophilic layer of poly(ethylene glycol) (PEG) have been used for the encapsulation and conjugation of doxorubicin and paclitaxel. Drug release in dependence of the pH was observed, and a greater efficiency of the nanocarriers in comparison to the free drug was additionally detected, due also to the combined effect of the two drugs.[15] A typical ligand for tumor targeting is represented by the peptide arginine-glycine-aspartate (RGD). In a recent work from Bi et al., doxorubicin was encapsulated in poly(lactide-co-glycolide) (PLGA) nanoparticles, which were firstly coated with dopamine and then functionalized with RGD and folate. A higher release could be observed at acidic pH in comparison to the neutral one, together with enhanced toxicity towards Hela cells and tumor targeting ability.[16]

Another biocompatible polymer is hyperbranched polyglycerol (hPG), [17] that finds extensive employment in the biomedical field due to its favorable characteristics such as the biocompatibility, the hydrophilicity, the low viscosity, and the presence of numerous terminal hydroxyl groups, which allow the easy functionalization of the polymer. For this reason, our group has used hPG for the development of both enzymatically and hydrolytically degradable prodrugs, in which methotrexate and doxorubicin were covalently attached to the polymeric structure.[18,19]

A major concern related to the use of hPG is, however, the possible accumulation of the compound in organs such as the liver and spleen, especially after the functionalization. Diverse approaches have therefore been used for the development of biodegradable nanocarriers based on hPG. As an example, via the copolymerization of glycerol and glycidyl methacrylate, ester bonds were introduced in the polymer, which ensure the biodegradability. Moreover, the anticancer drug methotrexate was chemically conjugated with the terminal groups of the polymer, resulting in an amphiphilic product that formed micelles in aqueous media. These could release the drug under acidic conditions and could inhibit the proliferation of diverse cell lines.[20] In another approach, the biodegradability was obtained thanks to the presence ketal moieties. The degradation profile *in vitro* and *in vivo* was examined, showing remarkable difference, probably due to the much more complex environment *in vivo*.[21] In order to enhance the biocompatibility, we have copolymerized hPG with a low amount of PCL and obtained a biodegradable nanocarrier (hPG-co-PCL), which has been loaded with the model dye Nile Red and has shown enhanced skin penetration, being therefore a promising candidate for the treatment of skin diseases.[22] Furthermore, its sulfate derivative ((hPG-co-PCL)S) has been shown to be able to bind to inflammatory mediators like selectins and to influence the activation of the complement system and therefore to possess high anti-inflammatory potential.[23]

The sulfation of the copolymer represent not only a crucial aspect for the employment in inflammatory states, but also in relation to the targeting of tumor tissue, which usually also shows inflammation. Recently, redox sensitive micelles composed of dendritic poly(glycerol sulfate) (dPGS) and PCL were synthesized and loaded with doxorubicin. This nanocarrier has shown extremely high targetability of the tumor *in vivo*, accompanied by a great antitumor performance.[24] Also, our group has presented a drug-conjugate composed of dPGS and monomethyl auristatin E (MMAE), which showed the potential in the employment of sulfated polymers for the targeting and the treatment of cancer. We have therefore focused our attention on the possibility of encapsulating an anticancer drug in the biodegradable copolymers hPG-co-PCL and (hPG-co-PCL)S. We now have

investigated the synthesis of these biodegradable copolymers in detail, to expand its understanding and application potential.

Here we present the upscaling of the synthesis of biodegradable hyperbranched copolymers based on hPG-co-PCL for the delivery of hydrophobic guests. We have considered parameters like monomer addition and temperature to study their effect on the polymerization. Moreover, we have investigated the suitability of the compounds as nanocarriers for hydrophobic guests. The loading capacity has been examined using both a NIR dye and the drug doxorubicin. The toxicity of the nude carrier and after guest encapsulation has been investigated using a cancer cell line, Hela. Furthermore, the targeting ability of the sulfated copolymers was tested *in vivo*. The biodegradable copolymers have been demonstrated to be accessible on a multigram scale with a straightforward approach and to be suitable hosts for the employment in the targeting of cancer and the delivery of chemotherapeutics.

2. Results and discussion

2.1 Synthesis and loading of the nanocarriers

2.1.1 Synthesis of hPG-co-PCL and (hPG-co-PCL)S

The necessity of synthetic approaches that enable the production of nanocarriers with low costs in high scale has persuaded us to further investigate the already reported synthesis of biodegradable hPG-co-PCL. We aimed to gain a deeper understanding, optimize the process, and to expand the employment as nanocarriers for the transport of bioactive compounds for the treatment of inflammatory states and cancer therapy.

A series of biodegradable (hPG-co-PCL)s were synthesized through $Sn(Oct)_2$-catalyzed ring-opening copolymerization of glycidol and ε-caprolactone by slow monomer addition in bulk. Parameters like the temperature and the rate of monomer addition were investigated to understand their role on the characteristics of the product. In Table 1 the reaction conditions are summarized. In

comparison to the previously published work,[22] the temperature was increased to 100 °C and the ratio of the monomers was set as 10:1 (Gly : Ɛ-CL).

Table 1. General conditions adopted for the synthesis of hPG-co-PCL. For each entry, the total volume of monomers and catalyst added are reported. The molecular weight (Mn, measured via GPC) and the polydispersity index of the obtained products are also listed.

Entry	Glycidol (mL)	Ɛ-Caprolactone (mL)	Catalyst (mL)	Rate (mL min^{-1})	Temperature (° C)	Mn (kDa)	PDI
A	45	7,5	2,4	0,036	100	60	1.32
B	45	7,5	1,8	0,09	100	35	1.49
C	45	7,5	1,8	0,1	100	20	1.32
D	45	7,5	1,8	0,2	100	36	1.47

The rate of monomers addition and the temperature appeared to be crucial parameters in controlling the molecular weight of the product. Molecular weights up to 20 kDa were reached when the reaction was performed at 50 °C. By increasing the temperature to 100 °C, it was possible reach three times higher molecular weights, up to 60 kDa. The increase in the temperature corresponded also to a decrease in the reaction time, from 48 h up to 8 h. Moreover, it was possible to observed that a slow monomer addition was essential for accessing higher molecular weights.

For ensuring a prolonged stirring of the reaction and to prolog the reactivity of the monomers, an external stirring motor was employed. The reactions were stopped as the maximal torque applied (57 Ncm) was achieved. The increasing torque applied was registered and plotted against the time, to observe the reaction profiles. Moreover, the correlation with the amount of monomer added to the solution was also taken in account (**Figure 1**).

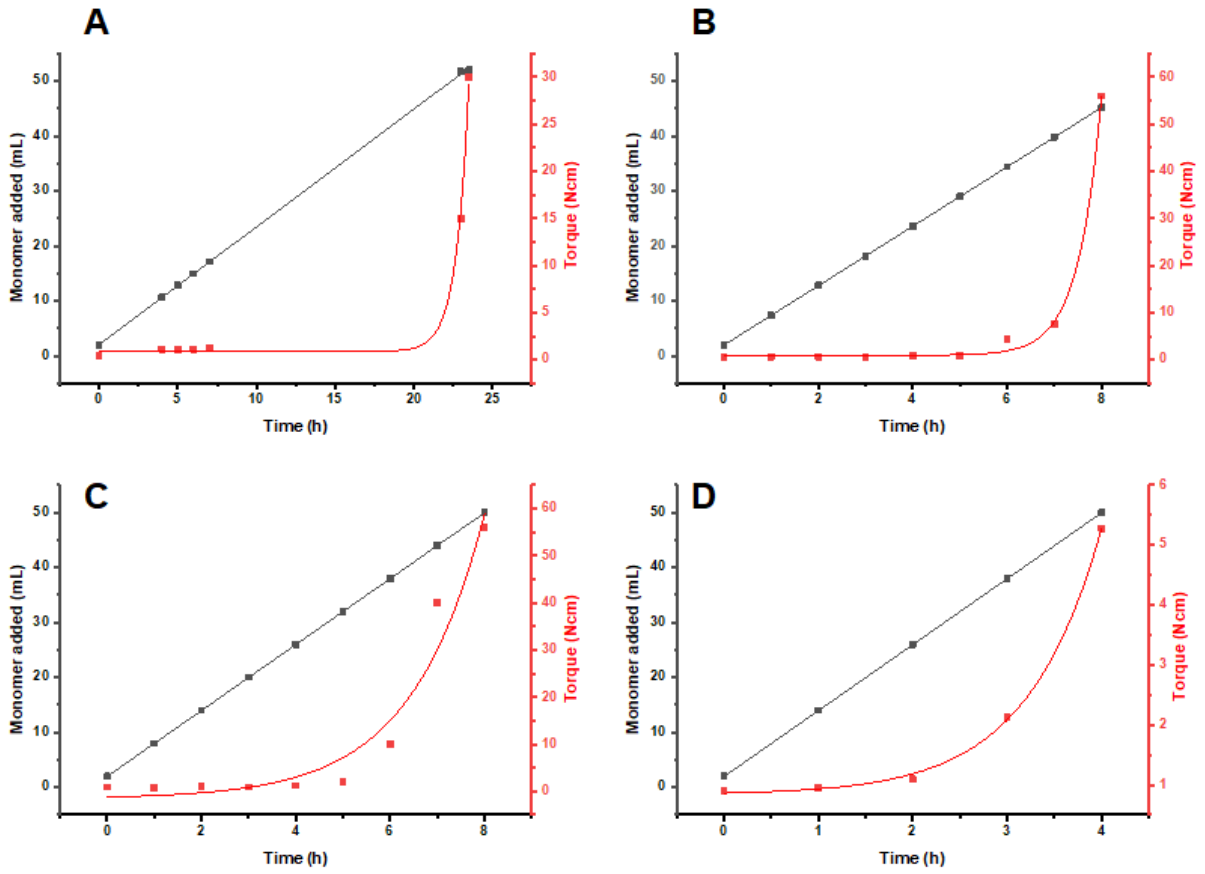

Figure 1. Plot of the viscosity of the reaction mixture and of the amount of monomer added against the time. The graphs display the torque's growth for the timeframe necessary for the monomers' addition. The plots are labelled in accordance to the entry of Table 1 (A, B, C, D).

It was possible to observe that the viscosity increased more quickly in correlation with the rate of the monomer addition. Moreover, also the graphs confirmed that a slow monomer addition approach was needed to delay the increase in the viscosity and to obtain a higher molecular weight. For a really slow monomer addition, the stirring was prolonged up to 24 h, while, in the case of a faster addition, the maximal torque applied was reached within 8 h.

The purification process was also optimized, as a tangential flow filtration (TFF) system replaced the previous dialysis approach. In comparison to the traditional method, a reduced amount of solvent was needed to clean the product, rendering the purification more environmentally friendly.

The time necessary to perform the purification was also reduced from 48 h up to 8 h. The pure product was obtained on a multigram scale up to 15 grams.

The degradability of the polymer via hydrolysis was confirmed upon storage in water for 3 months (pH = 6.5). Afterwards, the solvent was removed, and the molecular weight of the polymer investigated by gel permeation chromatography (GPC). As it can be seen in **Figure 2**, the polymer initially exhibited a quite narrow distribution, which was centered on a MW of 35 kDa. Afterwards, the polymer presented two distinct populations, mainly centered on the lower molecular weight compounds of 5 kDa. This result is in agreement with the studies previously reported for the polymers synthesized at lower temperature, where the stability at pH 5.4 and the degradation in the presence of a lipase were demonstrated for a timeframe of one week.[22]

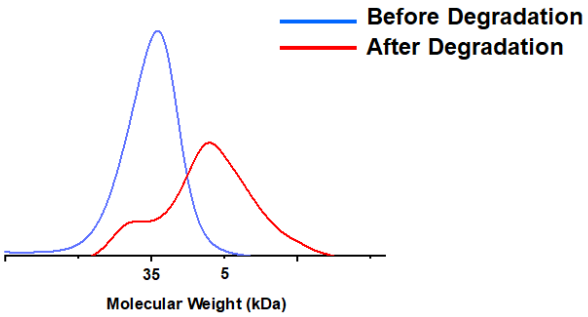

Figure 2. GPC profile before and after degradation via hydrolysis. A reduction of the molecular weight corresponding to 7-fold can be observed.

The above-described copolymers find potential employment in the delivery of anticancer drug to the tumoral tissue, because they possess a favorable size to be internalized via EPR effect. The metabolism of cancer cells is highly different from that of healthy tissue and is characterized by the development of own growth factors and angiogenesis.[25] These directly affect the morphology of the tissue, as it becomes unregular and more permeable to macromolecules, which usually cannot enter the tight healthy tissue. Moreover, due to the ineffective lymphatic drainage, the macromolecules will not be cleared but preferentially accumulate in the tumor.[10,26] Furthermore, the tendency to degrade

via hydrolysis suggests that, after the initial accumulation in the tumor, the carriers could be degraded and cleared from the body, thus preventing the risk of accumulation in the organs and rising of side effects.

2.1.2 Encapsulation experiments and size investigation

Two polymers were chosen for the sulfation and investigation as suitable nanocarriers for hydrophobic compounds. A low molecular weight copolymer (Mn = 17 kDa) obtained at 50 °C and a high molecular weight copolymer (Mn = 60 kDa) synthesized at 100 °C were compared.

The hydroxy terminal groups were converted in sulfates by the use of sulfur trioxide pyridine complex, in an overnight reaction at 60 °C. After the quenching of the reaction with NaOH, dialysis was performed to remove the remaining traces of pyridine. Degree of sulfation between 86% and 97% were estimated on the basis of the sulfur content of the functionalized polymers. Moreover, based on elemental analysis, it was also possible to calculate the molecular weight, which according to the theory, almost doubled for each product, when compared to the starting material. The characteristics of the polymers and their sulfated version are listed in the Table 2. The compounds used for the encapsulation tests are also listed.

Table 2. Polymers investigated as nanocarriers**.** The molecular weight of the sulfated compounds was calculated based on the elemental analysis. (n.d. not determined. LC loading capacity).

Compound class	Name	Molecular weight (Mn)	Degree of sulfation	Encapsulated compound and LC (wt %)
hPG-co-PCL OH	hPG-co-PCL_{17}	17 kDa	0 %	Doxo (14 %)
hPG-co-PCL S	hPG-co-$PCL_{17}S_{0.86}$	MW*: 37 kDa	86 %	Doxo (5%)
hPG-co-PCL S	hPG-co-$PCL_{60}S_{0.97}$	MW*: 127 kDa	97 %	Doxo (14%) S 0796 (n.d.)

In order to test the suitability of the copolymers as nanocarriers for drug delivery, the cytostatic doxorubicin was chosen for the encapsulation studies. The drug was physically entrapped in the copolymers using the film method. Briefly, after the formation of a film of guest in a small vial, a freshly prepared solution of polymer in distilled water was added and stirred overnight. After the removal of the free guest, the content of the drug was determined via UV-Vis spectroscopy.
The loading capacity of the copolymers was studied in relation to the molecular weight of the carrier and the degree of sulfation. The loading capacity is defined as the ratio of the guest amount to that of the carrier. The results are summarized in Table 2.

The encapsulation of doxorubicin into the copolymers hPG-co-PCL_{17}, hPG-co-$PCL_{17}S_{0.86}$, and hPG-co-$PCL_{60}S_{0.97}$ was successful. The great interaction of the copolymers with the Doxo might be accredited both to the presence of hydrophobic segments in the polymer and to the instauration of ionic interactions between the host and the guests. This appeared to be particularly relevant for the high molecular weight-sulfated compound, which presented a greater number of sulfates groups to interact with. The higher loading might also be attributed to the larger size of hPG-co-$PCL_{60}S_{0.97}$, which enabled the interaction of a greater number of doxorubicin molecules. To confirm this, the size of the nanoparticle before and after encapsulation of doxorubicin was investigated via dynamic light scattering (DLS) measurements in phosphate buffer (**Figure 3**).

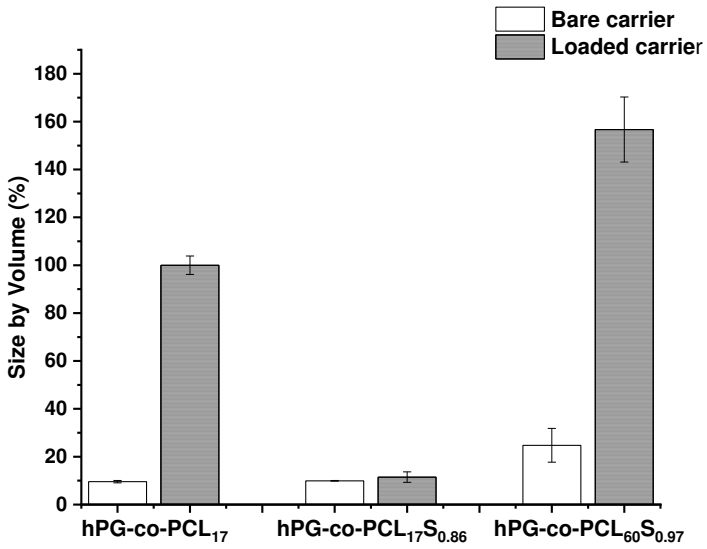

Figure 3. Size comparison before and after loading with doxorubicin in phosphate buffer solution.

All the three nanocarriers exhibited a size ranging between 9 and 25 nm prior the loading. It is possible to observe that, after the encapsulation of the drug, the size of the nanocarriers increased in accordance to the LC. For the smaller copolymer hPG-co-$PCL_{17}S_{0.86}$, an almost constant size is observed, which might be due to the restricted amount of encapsulated guests. On the contrary, the large presence of doxorubicin of the surface of hPG-co-PCL_{17} and hPG-co-$PCL_{60}S_{0.97}$ might have induced some aggregation.

2.2 In vitro and in vivo evaluation of the performance of the nanocarriers

2.2.1 Real time cell analysis

The surprising higher loading of the hPG-co-PCL_{17} in comparison to its derivative hPG-co-$PCL_{17}S_{0.86}$ advised the possible presence of free drug in the compound. The hPG-co-PCL_{17} could, in fact, not be purified via size exclusion chromatography, as some instability of the solution was displayed when the approach was tested. We therefore speculated on the possibility that the dialysis approach might have been only partially successful in removing the free drug. This assumption found confirmation

in the results of the real time cell analysis (RTCA). Hela cells were incubated with 20, 10, and 2 µM doxorubicin polymer solutions, and the viability was monitored for 24 h after administration.

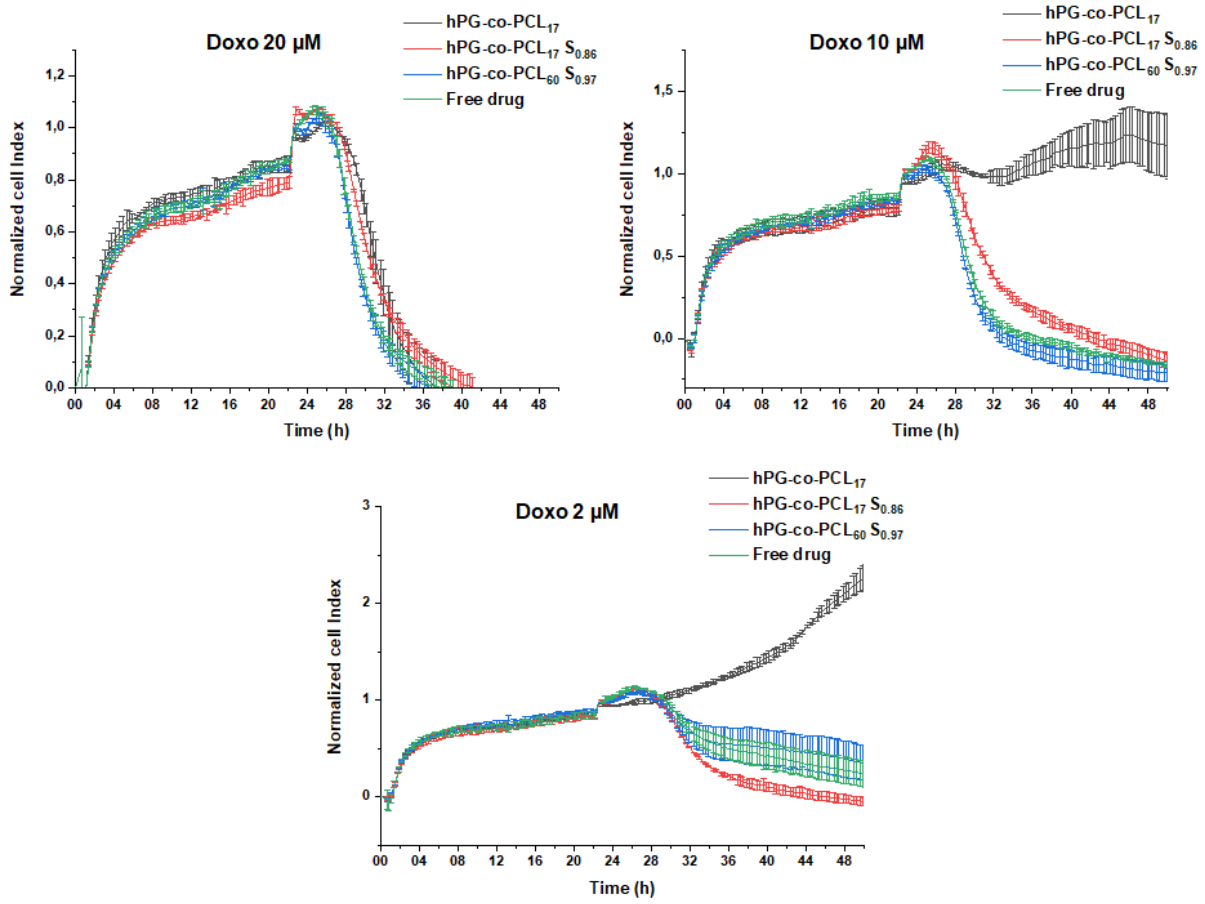

Figure 4. Real time cell analysis of the polymer loaded with doxorubicin. The cell proliferation was constantly monitored for 24 h after the treatment with the solution containing the drug. To enable the comparison, the nanocarrier solutions are calibrated on the drug content. Drug concentration range: 20 – 2 µM.

As depicted in **Figure 4**, the unsulfated copolymer hPG-co-PCL_{17} (in black) only showed efficient drug delivery when the doxorubicin concentration was equal to 20 µM. As the concentration of the drug decreased, the viability of the cells was not more affected. An increase in the viability was even detected, suggesting that the cytotoxic effect showed at 20 µM was due to some drugs that might still have been not physically bound to the nanocarrier. On the contrary, both the sulfated compounds (in red and blue) were able to release their cargo independently from the concentration. Moreover, at

the small concentration of 2 µM, the hPG-co-$PCL_{17}S_{0.86}$ (red) seemed to deliver the doxorubicin with a higher efficiency than that of the free drug (green).

2.2.2 Cytotoxicity assays

The biocompatibility of nanocarriers is an essential requisite for their employment. The previous works already demonstrated that the cell lines HaCaT, A549, and Caco-2 could tolerate the administration of the compounds. Here we describe the effect of the administration of a higher quantity of nanocarrier, in order to detect the toxic dose. The results are reported in **Figure 5**.

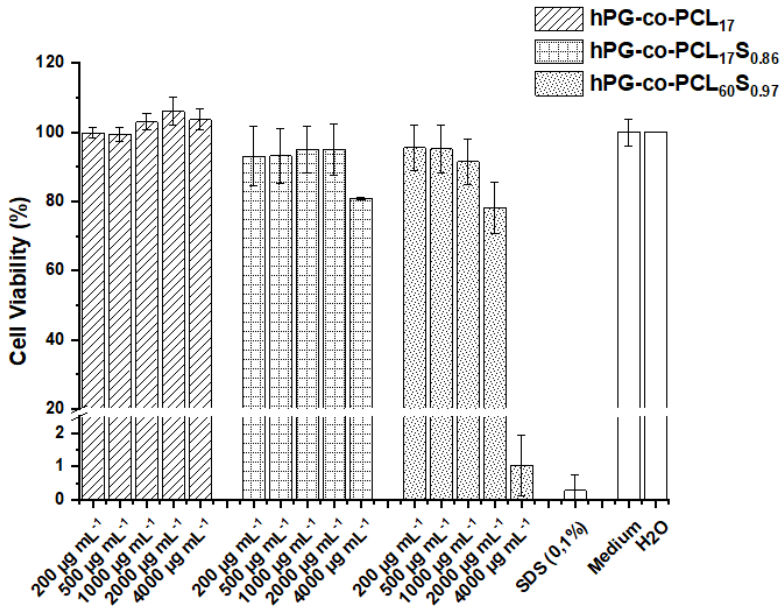

Figure 5. Maximum tolerated dose of the unloaded nanocarrier, investigated in a viability assay. (n = 3, for 4000 µg mL^{-1} n = 2)

The toxicity of the copolymer was investigated in the range 200 µg mL^{-1} to 4000 µg mL^{-1}. The cytotoxic effect of the compounds seems to be related to the size and the molecular weight of the administered copolymer. The high MW sulfated hPG-co-$PCL_{60}S_{0.97}$ reduced the cell viability to almost 78% when 2 mg mL^{-1} compound were administered, while the viability increased to 91% at the lower concentration of 1 mg mL^{-1}. The hPG-co-$PCL_{60}S_{0.97}$ showed a remarkable toxic effect only

at the really high concentration of 4 mg mL^{-1}, at which less than 2% of the cells could survive. The smaller sulfated hPG-co-$PCL_{17}S_{0.86}$ reduced the viability to a maximum of 80%, while the hPG-co-PCL_{17} seemed not to affect the cells even at high concentrations.

To confirm the trend displayed by the RTCA, we have investigated the cytotoxicity of the nanocarriers loaded with Doxo also in a viability assay. The results are depicted in **Figure 6.**

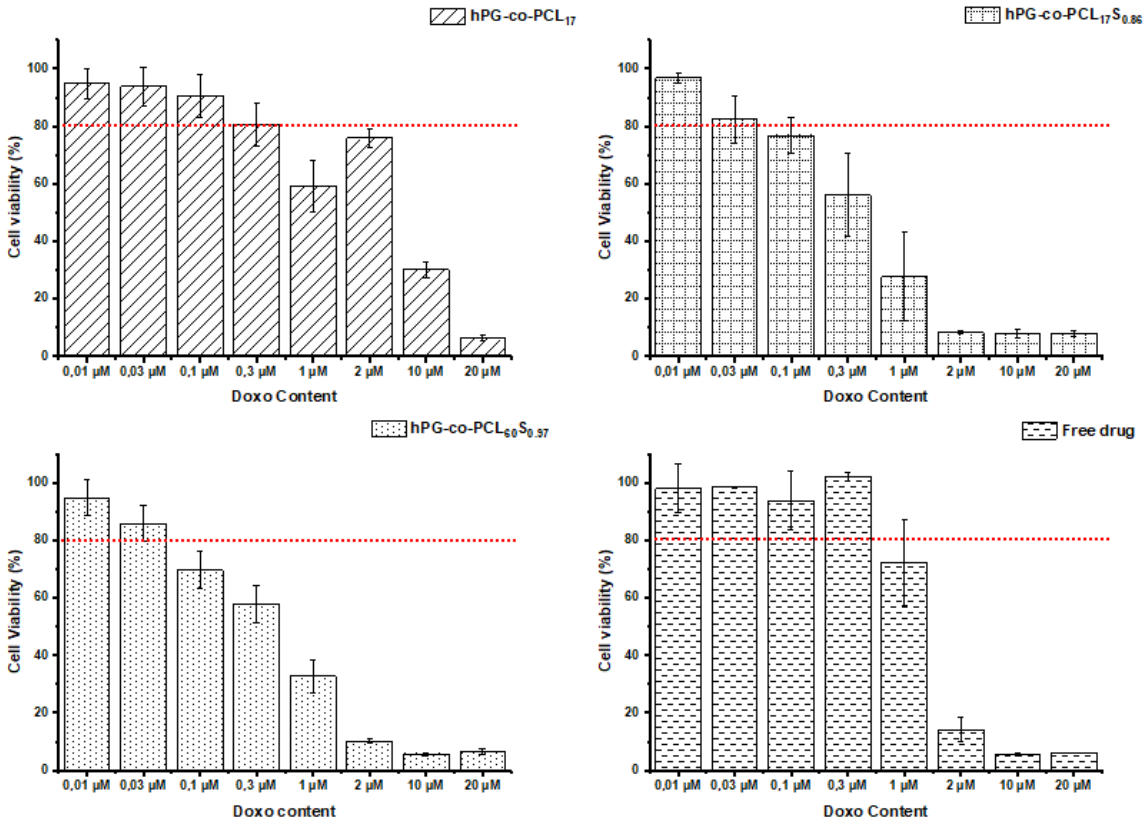

Figure 6. Cytotoxicity assay performed with the nanocarriers loaded with doxorubicin, in the concentration range 0,01 µM to 20 µM. (n = 3, for doxo 0,03 µM and 0,3 µM n = 1)

After loading the carriers, solutions containing 0,01 to 20 µM Doxo were administered to the cells, to investigate the capability of the nanocarriers in delivering and releasing the drug. It is possible to observe that, in agreement with the RTCA data, only the sulfated compounds could efficiently deliver the drug to the cells, even at low doxorubicin concentrations. The free drug displayed cytotoxic effects in the concentration range 2 µM to 20 µM. At the concentration 1 µM, it is possible

to observe that the non-toxic limit (80 % viability) is included in the error range, suggesting that the drug might be non-effective. On the contrary, at the same drug concentration (1 μM), a reduction in the cell viability to 30 % was observed when the Doxo was administered with the sulfated nanocarriers. The same trend could be observed with the lower concentrations 0,3 μM and 0,1 μM, remarking the enhanced efficiency of the nanocarriers in comparison to the free drug. For Doxo concentration lower than 0,03 μM, the viability resulted not more affected, neither by the drug nor the loaded nanocarriers. Noteworthy, due to the different loading capacity of the sulfated polymers (4 % vs 14 %), a much higher amount of hPG-co-$PCL_{17}S_{0.86}$ compared to hPG-co-$PCL_{60}S_{0.97}$ was needed to deliver the same amount of doxorubicin. Moreover, for the delivery of a drug concentration equal to 2 μM, only 10 μg mL^{-1} of the carrier hPG-co-$PCL_{60}S_{0.97}$ were needed, which is almost 400-fold less than its toxic concentration. Therefore, the hPG-co-$PCL_{60}S_{0.97}$ resulted to be a better candidate as a drug nanocarrier, as a smaller amount of polymer was needed to efficiently transport the drug, which potentially results in less side effects due to the nanocarrier itself.

2.2.3 Encapsulation of a NIR dye and in vivo distribution

Since the tumor is usually accompanied by inflammation and previous works showed the high binding affinity of sulfated polyglycerols to the inflamed cells and the targeting of tumor *in vivo* using sulfated micelles, [23,24,27] we aimed to test the targetability of the new nanocarriers towards solid tumors. The ability of the sulfated compound to target the cancer environment was tested *in vivo*. The best carrier for the encapsulation of doxorubicin, namely, hPG-co-$PCL_{60}S_{0.97}$, was employed for the physical loading with the cyanine dye S 0796.

A solution containing the nanocarrier loaded with the NIR dye was injected in nu/nu mice bearing HT29 tumors, either intravenously (i.v.) or subcutaneously (s.c), and the biodistribution was observed for 24 h, at regular intervals, via fluorescence microscopy. The results after 24 h administration are reported in **Figure 7**.

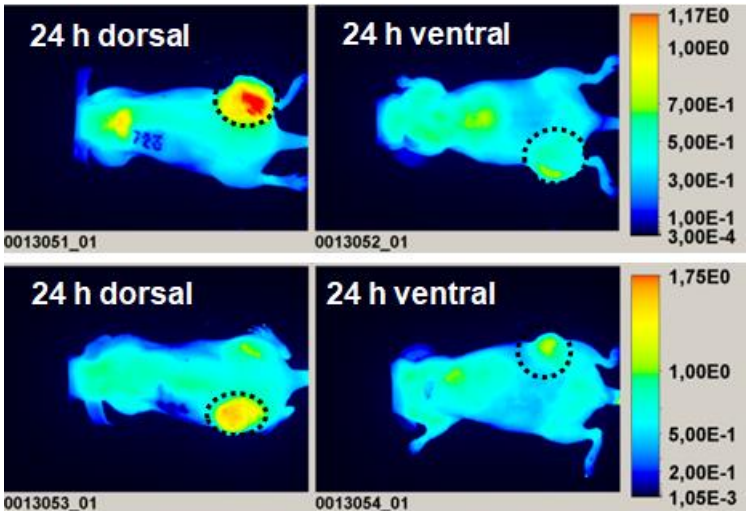

Figure 7. *In vivo* tumor targeting tests with mice bearing HT29 tumors. The reported results correspond to the imaging 24 h after injection. On the top, intravenous injection, on the bottom subcutaneous injection. The tumor is circled in black. (n = 1)

After 24 h tail injection, a strong accumulation in the tumor tissue can be observed in both the cases. The positive results confirmed the ability of sulfated nanocarrier to target the cancer environment and to accumulate preferentially at the tumor site. Moreover, the efficient targeting after both intravenous and subcutaneous injection suggests that the nanocarriers are potentially suitable for diverse administration approaches. This opens the way to the preclinical development of a new biodegradable polyglycerol-co-polycaprolactone nanocarrier for tumor therapy.

3. Conclusions

In this work we have presented the possibility to upscale the synthesis of the biodegradable (hPG-co-PCL)s and their employment as nanocarriers for hydrophobic compounds.

The rate of monomers' addition was a crucial parameter in controlling the molecular weight of the copolymer. Moreover, an increase in the temperature of the reaction corresponded to a reduction in the time necessary to form the product and higher molecular weights could be obtained. Furthermore, it was shown that the purification of the product could easily be performed using a tangential flow filtration system instead of the common dialysis approach, resulting in a less time and

resource-consuming method. Furthermore, the degradability of the polymer was confirmed by incubation in water over 3 months.

The suitability of the biodegradable copolymers and their sulfated derivatives as nanocarriers was tested using the anticancer drug doxorubicin, and a high loading was observed, especially for hPG-co-$PCL_{60}S_{0.97}$ (14 wt%). Both the sulfated copolymers efficiently delivered their cargo to the tumor cell line Hela, demonstrating an enhanced effect in comparison to the free drug at lower concentrations, therefore confirming their potential as nanocarriers. Moreover, the best performing hPG-co-$PCL_{60}S_{0.97}$ was loaded with an NIR dye and tested *in vivo* regarding the biodistribution and targeting ability of cancer. After 24 h tail injection, the nanocarrier preferentially accumulated in the tumor, demonstrating the affinity of sulfated compound to cancer tissue. Moreover, both the intravenous and subcutaneous injection led to comparable results. These findings represent a first proof of concept for the development of biodegradable nanocarriers, accessible via a straightforward approach on a multigram scale, which find potential application in the target delivery of chemotherapeutic agents.

4. Experimental session

4.1 Materials and methods

Chemicals were reagent grade, purchased from Acros Organics, Sigma Aldrich, and Carl Roth, and were used without further purification. Glycidol and Ɛ-caprolactone were purchased from Acros and used after distillation. Dialysis was performed using either benzoylated cellulose membrane (Sigma) or regenerate cellulose membrane (Roth).

Tangential flow filtration was performed using a 30 kDa regenerated cellulose cassette (Merck) in a cassette holder (Sartorius). The flow of the solution through the system was induced by a peristaltic pump (Gibson). The flow rate was kept at the maximal one. (30 mL min^{-1})

^{1}H and ^{13}C NMR and were recorded either on a Bruker AVANCE III 500 (Bruker Corporation), or a Jeol ECP 500 (JEOL GmbH), or a Bruker AVANCE III 700 (Bruker Corporation). Deuterated solvents were used as internal standards and chemical shifts δ reported in ppm.

Elemental analysis (EA) was performed with a VARIO EL (Elementar).

Gel permeation chromatography (GPC) measurements were performed in water, using an Agilent 1100 (Agilent Technologies). The instrument was equipped with a manual injector, an isopump and a differential refractometer. For the separation of the samples, three columns of 30 cm were used. Measurements were conducted at room temperature, using 100 µL of solution at a concentration 5 mg/mL.

The particle size was determined via dynamic Light Scattering (DLS) measurements, which were carried out on a Zetasizer Ultra (Malvern Instruments Ltd.) equipped with a He-Ne laser (nm). Backscattering mode was employed (detector angle 173°). Samples were dissolved in water, at a concentration of 1 mg mL^{-1} and filtered with 0.45 µm regenerated cellulose (RC) syringe filter prior measurement. UV-transparent disposable cuvettes (Plastibrand microcuvette) were used. For each measurement, 13 scans per samples were taken.

UV measurements were conducted on an Agilent Cary 8454 UV-visible spectrophotometer, using half-micro quartz cuvettes.

4.2 Synthesis of hPG-co-PCL and hPG-co-(PCL)S

Hyperbranched polyglycerol-co-polycaprolactone and their sulfated derivatives were prepared adapting the protocols previously reported by our group.[22,23]

hPG-co-PCL was obtained via copolymerization of glycidol and Ɛ-caprolactone, in the presence of tin octoate as the catalyst. By varying the temperature (50 °C to 100 °C), time of the reaction (8 to 48 h), and the rate of the monomer addition, products with different molecular weights on diverse gram scales (10 to 15 g) were obtained. As an example, in a 750 mL reactor equipped with an external mechanical stirrer, 360 µL $Sn(Oct)_2$ were placed, the reactor evacuated three times and

filled with nitrogen. Glycidol (45 ml, 0,68 mol) and Ɛ-caprolactone (7,5 ml, 0,068 mol) were mixed in a syringe, 2 mL solution was inserted in the flask, and the rest was added by slow monomer addition. Aliquots of the catalyst was added every 2 h, at a volume of 360 μL each time, until the targeted amount was reached (Table 1). The reaction was quenched with MeOH if the stirring was not possible.

After purification by dialysis or tangential flow filtration, the hydroxyl terminal groups were converted to sulfate via overnight reaction with sulfur trioxide pyridine complex (1,5 eq/OH), at 60 °C. The reaction was carefully quenched using NaOH 1 M and the pH was adjusted to 7.4. The purification was then performed via dialysis, and the medium was changed from brine to water decreasing the salt concentration step by step.

4.3 Encapsulation of doxorubicin

For the encapsulation of the drug, the film method[28] was employed.

Doxorubicin HCl (abcr GmbH) was converted to the more hydrophobic free base prior to employment, by extraction with chloroform after the addition of triethyl amine (4 eq). Doxorubicin was then dissolved in MeOH (pharmaceutical grade), a small volume (50 wt% drug) was transferred in a vial and the solvent was carefully removed at the rotatory evaporator, in order to get a regular film. 2 mL of a stock solution of polymer (c = 5 mg mL^{-1}) in distilled water were added, and the solution was stirred at 1200 rpm overnight.

For the separation of the free drug, different methodologies based on the MW of the host were employed. Sephadex G75 in water was performed on the high molecular weight-sulfated samples (MW = 125 kDa), while the smaller ones (MW = 40 kDa) were passed on Sephadex G25. The unsulfated polymers were dialyzed with a Slide-A-Lyzer™ MINI Dialysis Device (ThermoFischer) (cut off 3,5 kDa) for 18 h. The amount of encapsulated guest was determined via UV-Vis spectroscopy. As reference, a calibration curve in water-methanol (60:40) was taken (Doxo: λ = 499 nm). The loading capacity (LC) of the nanocarriers was calculated using equation 1.

$$LC = \frac{mass(guest)}{mass\ (carrier)} * 100 \qquad \text{(Equation 1)}$$

4.4 Real Time Cell Analysis

For a real-time cell analysis (RTCA), 90 µl of Hela cell (DSMZ no.: ACC 57) suspension was seeded in a 96-well E-plate at a density of 100,000 cells mL^{-1} and placed in the xCELLigence real-time cell analyzer SP from Roche (Mannheim, Germany) at 37 °C and 5% CO_2 and impedance was measured at least every 15 minutes.

After 24 h incubation, 10 µl of hPG-co-PCL_{17}, hPG-co-$PCL_{17}S_{0.86}$ and hPG-co-$PCL_{60}S_{0.97}$ containing doxorubicin were added. The solutions were prepared on the basis of the doxorubicin content to obtain final concentrations of 20, 10, and 2 µM Doxo. Free drug at the same concentrations was also added to compare the performance. Non-treated cells and cells treated with SDS (1% and 0,1%) served as controls. After addition of the compounds, the real-time impedance measurement was continued for another 72 hours. Data from the RTCA software were exported and analyzed using the origin software.

4.5 Cytotoxicity assay

The cytotoxicity of the polymers before and after loading with doxorubicin was investigated using Hela cells (DSMZ no.: ACC 57). Hela cells were cultured in RPMI Media 1640 medium supplemented with L- glutamine, 100 U mL^{-1} penicillin, 100 µg mL^{-1} streptomycin and 10% fetal calf serum. The cells were stored at 37 °C with 5% CO_2 and subcultured twice a week.

The determination of the cell viability was performed using a CCK-8 Kit (Sigma-Aldrich), according to the manufacturer's instructions. 90 µl of cell suspension was seeded in a 96-well plate at a density of 50,000 cells mL^{-1} and incubated at 37 °C and 5% CO_2 overnight. Serial dilutions of samples were prepared in water and added to the cells (10µl/well). SDS (1% and 0.1%) and non-treated cells (10% water and media) served as controls. For the subtraction of the background, wells containing no cells but only samples were used. The CCK8 solution was added after 48 h incubation

and the absorbance (450 nm, reference: 650 nm) was measured after approximately 2 h using a Tecan plate reader (Infinite pro200, TECAN-reader Tecan Group Ltd.)

Measurements were performed in triplicates and repeated three times. The cell viability was calculated after subtracting the background signal by setting the non-treated control (10% water) to 100% and the non-cell control to 0%. The protocol was used for the investigation of the toxicity of the copolymer and of the loaded nanoparticles.

4.6 Encapsulation of a NIR dye and in vivo targeting test

For the *in vivo* experiments, the cyanine dye 2-[2-[2-Chloro-3-[2-(1,3-dihydro-1,3,3-trimethyl-2H-indol-2-ylidene)-ethylidene]-1-cyclohexen-1-yl]-ethenyl]-1,3,3-trimethyl-3H-indolium iodide (S0796, Few Chemicals) was chosen.

The previously described film method was used also for the encapsulation of the NIR dye. As a much lower amount of guest is required for imaging purposes, a film of 0,160 g dye was employed for the encapsulation in 2 mg of hPG-co-$PCL_{60}S_{0.97}$. After stirring for 18 h, the solution was placed in a Centriprep (cut off 10 kDa) and centrifuged for 1 h at 5000 rpm. The supernatant was then washed with fresh water and centrifuged again for 1 h. The dye content was determined per UV/Vis spectroscopy, using a calibration curve of the guest in water-ethanol (50:50) as reference (λ = 776 nm).

For the targeting *in vivo*, nu/nu mice carrying HT29 tumors were chosen and 100 µL with a dye-carrier concentration of 5 nM were injected in the tail, either intravenous (i.v.) or sub cutaneous (s.c.).

The imaging was performed under isoflurane anesthesia at 10 min, 40 min, 1 h, 3 h, 6 h, and 24 h on Pearl imager (800 nm channel, 85 µm resolution). Images were all set to equal scale for a mouse.

Acknowledgment

We acknowledge Isabelle Heing-Becker and the company Few Chemicals for providing the NIR dye, Cathleen Schlesener for GPC measurements, and Dr. Pamela Winchester for language polishing the article. We would like to acknowledge the SFB 765 and the Focus Area Nanoscale for the financial support.

Magda Ferraro and Ehsan Mohammadifar equally contributed to this work.

References

[1] R. Haag, F. Kratz, *Angew. Chemie Int. Ed.* **2006**, *45*, 1198.

[2] F. Yamashita, M. Hashida, *Adv. Drug Deliv. Rev.* **2013**, *65*, 139.

[3] M. Krischke, G. Hempel, S. Völler, N. André, M. D'Incalci, G. Bisogno, W. Köpcke, M. Borowski, R. Herold, A. V. Boddy, J. Boos, *Cancer Chemother. Pharmacol.* **2016**, *78*, 1175.

[4] R. Thorn, Caroline; Oshiro, Connie; Marsh, Sharon; Hernandez-Boussard, Tina; McLeod, Howard; Klein, Teri; Altman, *Pharmacogenet Genomics* **2012**, *21*, 440.

[5] D. Zhang, Q. Xu, N. Wang, Y. Yang, J. Liu, G. Yu, X. Yang, H. Xu, H. Wang, *Int. J. Nanomedicine* **2018**, *Volume 13*, 4549.

[6] J. Khandare, M. Calderón, N. M. Dagia, R. Haag, *Chem. Soc. Rev.* **2012**, *41*, 2824.

[7] L. Arms, D. W. Smith, J. Flynn, W. Palmer, A. Martin, A. Woldu, S. Hua, *Front. Pharmacol.* **2018**, *9*, 1.

[8] E. Fleige, M. A. Quadir, R. Haag, *Adv. Drug Deliv. Rev.* **2012**, *64*, 866.

[9] D. Rosenblum, N. Joshi, W. Tao, J. M. Karp, D. Peer, *Nat. Commun.* **2018**, *9*, DOI 10.1038/s41467-018-03705-y.

[10] H. Maeda, H. Nakamura, J. Fang, *Adv. Drug Deliv. Rev.* **2013**, *65*, 71.

[11] Q. Feng, R. Tong, *Bioeng. Transl. Med.* **2016**, *1*, 277.

[12] E. Gillies, J. Frechet, *Drug Discov. Today* **2005**, *10*, 35.

[13] F. Fouladi, K. J. Steffen, S. Mallik, *Bioconjug. Chem.* **2017**, *28*, 857.

[14] R. Ferrari, M. Sponchioni, M. Morbidelli, D. Moscatelli, *Nanoscale* **2018**, *10*, 22701.

[15] H. He, Y. Wang, H. Wen, X. Jia, *RSC Adv.* **2014**, *4*, 3643.

[16] D. Bi, L. Zhao, R. Yu, H. Li, Y. Guo, X. Wang, M. Han, *Drug Deliv.* **2018**, *25*, 564.

[17] S. Abbina, S. Vappala, P. Kumar, E. M. J. Siren, C. C. La, U. Abbasi, D. E. Brooks, J. N. Kizhakkedathu, *J. Mater. Chem. B* **2017**, *5*, 9249.

[18] M. Calderón, R. Graeser, F. Kratz, R. Haag, *Bioorg. Med. Chem. Lett.* **2009**, *19*, 3725.

[19] M. Calderón, P. Welker, K. Licha, I. Fichtner, R. Graeser, R. Haag, F. Kratz, *J. Control. Release* **2011**, *151*, 295.

[20] M. Hu, M. Chen, G. Li, Y. Pang, D. Wang, J. Wu, F. Qiu, X. Zhu, J. Sun, *Biomacromolecules* **2012**, *13*, 3552.

[21] R. A. Shenoi, S. Abbina, J. N. Kizhakkedathu, *Biomacromolecules* **2016**, *17*, 3683.

[22] E. Mohammadifar, F. Zabihi, Z. Tu, S. Hedtrich, A. Nemati Kharat, M. Adeli, R. Haag, *Polym. Chem.* **2017**, *8*, 7375.

[23] M. Ferraro, K. Silberreis, E. Mohammadifar, F. Neumann, J. Dernedde, R. Haag, *Biomacromolecules* **2018**, *19*, 4524.

[24] Y. Zhong, M. Dimde, D. Stöbener, F. Meng, C. Deng, Z. Zhong, R. Haag, *ACS Appl. Mater. Interfaces* **2016**, *8*, 27530.

[25] D. Hanahan, R. A. Weinberg, *Cell* **2000**, *100*, 57.

[26] I. N. Kurniasih, J. Keilitz, R. Haag, *Chem. Soc. Rev.* **2015**, *44*, 4145.

[27] T. Ji, Y. Zhao, Y. Ding, G. Nie, *Adv. Mater.* **2013**, *25*, 3508.

[28] E. Fleige, K. Achazi, K. Schaletzki, T. Triemer, R. Haag, *J. Control. Release* **2014**, *185*, 99.

4 Summary and Outlook

The increasing need to provide more efficient delivery of drugs for different illnesses is a key topic in the biomedical field. Synthetic polymers find wide employment in the development of diverse tools that perform their activity on the disease or can help to deliver small molecules like drugs to the desired site of action.

In this thesis, biodegradable polyglycerol-based polymers for the treatment of inflammatory diseases and the delivery of hydrophobic guests were presented. Hyperbranched polyglycerol, which is a highly biocompatible polymer, with easy synthesis, hydrophilic character, and numerous end groups suitable for further functionalization, was chosen to develop new biodegradable compounds. The copolymerization of glycidol with Ɛ-caprolactone resulted in a biodegradable version of the well-established hyperbranched polyglycerol (hPG), thanks to the presence of ester bonds in the backbone. The copolymer has been further functionalized, characterized, and studied *in vitro* regarding its biocompatibility, biodegradability, and suitability for the application in the biomedical field.

In the first project, this new copolymer was functionalized to obtain a biodegradable sulfated derivate ((hPG-co-PCL)S), which has been investigated for possible applications in the treatment of inflammatory states. Previous studies have highlighted the high affinity of dendritic polyglycerol sulfate (dPGS) to L-selectin but also demonstrated its accumulation in organs such as the spleen and liver, remarking the necessity of biodegradable compounds for *in vivo* applications. In this work, it was observed that the biodegradable version of dPGS is a valid alternative to the well-established one and, depending on the molecular weight and the degree of sulfation, it was possible to achieve diverse performance profiles concerning the inhibition of the binding of L-selectin towards its ligands, a crucial step in the recruitment of leukocytes to the site of inflammation. The (hPG-co-PCL)S was also capable to reduce the activity of the complement system, showing at the same time only a restrained effect on blood coagulation. Moreover, the new copolymer was biodegradable and had low cytotoxicity, before and after degradation, which was demonstrated with different cell lines.

In the second project, the biodegradable hPG-co-PCL was used as macroinitiator for the synthesis of pH responsive nanocarrier for the treatment of pancreatic cancer. It is well established that, while the human body generally presents a neutral pH, the cancer is characterized by a local acidic pH. This feature can be employed to induce the release of the guest molecules only at the desired site of action. The hPG-co-PCL core was used to graft a polycarbonate block, which was further functionalized with a tertiary amine, namely, N,N'-dibutylethylene diamine. The new

polymer was used both for the covalent conjugation and physical encapsulation of the anticancer drug gemcitabine (GEM). The nanocarrier was able to deliver its cargo in a pH-dependent fashion, with different rates depending on the type of loading.

In the third project, the upscaling of the synthesis of hPG-co-PCL and its employment as a nanocarrier for hydrophobic guests, both before and after sulfation, was investigated. The parameters, which govern the synthesis of the hPG-co-PCL, were inspected to determine the conditions that lead to different molecular weights while improving the gram scale of the product. The production on large scale at low costs is a primary need to access the market. Moreover, the relationship between tumor and inflammation is generally accepted. The dPGS has already demonstrated to be capable of targeting the tumoral environment, which suggests using new above-mentioned nanocarriers for the delivery of anticancer drugs. Two possible guests were physically encapsulated in the biodegradable copolymers: the anticancer drug doxorubicin, and a near infrared (NIR) dye. A great interaction both with doxorubicin and the dye was observed. The sulfated compounds displayed the best capacity of delivering the guest to the tumor cell line Hela *in vitro*, with increased performance depending on the molecular weight and correlating loading capacity. Moreover, the best candidate for the delivery of doxorubicin was loaded with the hydrophobic NIR dye S 0796 and tested *in vivo* to explore the capacity of the polymer in targeting the tumor. Accumulation in the tumor was observed 24 h after the injection, confirming the affinity of the sulfated compound to inflamed and cancerous tissue. These preliminary results show the potential for the employment of the new biodegradable sulfated nanocarriers for tumor therapy.

These outcomes describe the potential of the new nanocarriers for biomedical application, but further studies are needed to expand these findings. *In vivo* studies, which demonstrate the stability of the nanocarriers in the blood stream and a sufficient circulation time, would be necessary to confirm their suitability as nanocarriers. Due to the large diversity of anticancer drugs, a screening of the possible guests should be performed to determine which cancer type represents an appropriate target for the above-presented nanocarriers. The increase in the hydrophobic caprolactone component might be taken in account to ensure a better loading capacity of small molecules like dexamethasone. The influence of the encapsulation method, namely the conjugation in comparison to the physical entrapment, of both the anticancer drugs and NIR dye should be studied to understand its role on the drug delivery *in vivo*. Moreover, the possibility to use the new biodegradable carriers for theranostics applications shall be further explored.

5 Zusammenfassung

In dieser Arbeit wurden biologisch abbaubare Polymere auf Polyglycerin-Basis für die Behandlung von Entzündungskrankheiten und die Freisetzung von hydrophoben Molekülen, wie Therapeutika oder Farbstoffen, vorgestellt. Hyperverzweigtes Polyglycerin (hPG) wurde als Kandidat für die Entwicklung neuer bioabbaubarer Polymere ausgewählt. Dieses ist ein biokompatibles Polymer, welches leicht zu synthetisieren ist, und einen hydrophilen Charakter und zahlreiche terminale, funktionalisierbare Hydroxygruppen besitzt. Die Copolymerisation von Glycidol mit Ɛ-Caprolacton führte, auf Grund der Esterbindungen im Polymerrückgrat, zu einer biologisch abbaubaren Version des etablierten hPG. Das Copolymer wurde weiter funktionalisiert, charakterisiert und *in vitro* in Bezug auf seine Biokompatibilität, Bioabbaubarkeit und Eignung für die Anwendung im biomedizinischen Bereich hin untersucht.

Im ersten Projekt wurde dieses neue Copolymer funktionalisiert, um ein biologisch abbaubares, sulfatiertes Derivat ((hPG-co-PCL)S) zu erhalten, das auf den möglichen Einsatz bei der Behandlung von Entzündungszuständen hin untersucht wurde. Frühere Studien haben die hohe Affinität von dendritischem Polyglycerinsulfat (dPGS) zu L-Selektin, jedoch auch ihre Akkumulation in Organen wie Milz und Leber gezeigt. In dieser Arbeit wurde festgestellt, dass es je nach Molekulargewicht und Sulfatierungsgrad möglich ist, unterschiedliche Leistungsprofile bezüglich der Hemmung der Bindung von L-Selektin an ihre Liganden zu erreichen, was einen entscheidenden Schritt bei der Rekrutierung von Leukozyten an den Entzündungsort darstellt. Die hPG-co-PCLS Polymere waren auch in der Lage, die Aktivität des Komplementsystems zu reduzieren und haben gleichzeitig nur einen geringen Einfluss auf die Blutgerinnung gezeigt. Darüber hinaus konnte gezeigt werden, dass das neue Copolymer enzymatisch abbaubar ist und eine geringe Zytotoxizität, sowohl vor als auch nach dem Abbau, aufweist.

Im zweiten Projekt wurde das biologisch abbaubare hPG-co-PCL als Makroinitiator für die Synthese von pH-sensitiven Nanocarriern zur Behandlung von Bauchspeicheldrüsenkrebs eingesetzt. Der menschliche Körper hat normalerweise einen neutralen pH-Wert, aber im Fall von Krankheiten wie Krebs, kann lokal ein saurer pH-Wert auftreten. Durch pH-labile Nanocarrier wird die Freisetzung des Gastmoleküls am gewünschten Wirkungsort initiiert. Mit dem hPG-co-PCL-Kern wurde ein Polycarbonatblock gepfropft, der mit einem tertiären Amin, nämlich N,N'-Dibutylethylendiamin (DB), weiter funktionalisiert wurde. Der neue Nanocarrier wurde sowohl für die kovalente Konjugation als auch für die physikalische Verkapselung des Krebsmedikaments Gemcitabin eingesetzt. Der neue Nanocarrier war in der Lage, seine Ladung pH-abhängig freizusetzen, wobei die Freisetzungsrate von der Beladungsart abhängig war.

Im dritten Projekt wurde der Einsatz von hPG-co-PCL, sowohl vor als auch nach der Sulfatierung, als Nanocarrier für hydrophobe Gäste untersucht. Zuerst wurde die Synthese des hPG-co-PCL genauer untersucht, um die Bedingungen zu bestimmen, die das Molekulargewicht und gleichzeitig die Ausbeutel des Produktes kontrollieren. Danach wurden zwei verschiedene hydrophobe Moleküle verkapselt: das Krebsmedikament Doxorubicin und der nahinfrarote Farbstoff S 0796. Eine große Interaktion mit Doxorubicin wurde beobachtet. Dabei zeigten die sulfatierten Derivate den größten Effekt in Bezug auf Freisetzung von Doxorubicin in der Tumorzelllinie Hela. Des Weiteren konnte eine Abhängigkeit der Wirksamkeit des Carriers vom Molekulargewicht und dessen Beladungsgrad observiert werden. Darüber hinaus wurde der beste Kandidat mit dem hydrophoben NIR-Farbstoff S 0796 beladen und *in vivo* in Mäusen die Fähigkeit des Polymers im Tumor zu akkumulieren, untersucht. Die Verteilung des Farbstoffes wurde 24 Stunden nach der Injektion untersucht, wobei eine Ansammlung im Tumor beobachtet werden konnte, was für die Affinität der sulfatierten Polymere zu entzündetem und krebsartigem Gewebe spricht. Diese Ergebnisse zeigen das Potential des Nanocarriers für den Einsatz im Tumor- und Entzündungstargeting.

6 References

[1] R. P. Tracy, *Int. J. Obes.* **2003**, *27*, 29–34.

[2] S. Shalapour, M. Karin, *J. Clin. Invest.* **2015**, *125*, 3347–3355.

[3] F. L. Heppner, R. M. Ransohoff, B. Becher, *Nat. Rev. Neurosci.* **2015**, *16*, 358–72.

[4] S. Mignani, S. El Kazzouli, M. Bousmina, J. P. Majoral, *Adv. Drug Deliv. Rev.* **2013**, *65*, 1316–1330.

[5] X. Pang, X. Yang, G. Zhai, *Expert Opin. Drug Deliv.* **2014**, *11*, 1075–1086.

[6] M. Beck-Broichsitter, J. Nicolas, P. Couvreur, *Eur. J. Pharm. Biopharm.* **2015**, *97*, 304–317.

[7] J. K. Patra, G. Das, L. F. Fraceto, E. V. R. Campos, M. del P. Rodriguez-Torres, L. S. Acosta-Torres, L. A. Diaz-Torres, R. Grillo, M. K. Swamy, S. Sharma, S. Habtemariam, H-S. Shinet, *J. Nanobiotechnology* **2018**, *16*, 71.

[8] U. Ikoba, H. Peng, H. Li, C. Miller, C. Yu, Q. Wang, *Nanoscale* **2015**, *7*, 4291–4305.

[9] R. Duncan, *Curr. Opin. Biotechnol.* **2011**, *22*, 492–501.

[10] E. Markovsky, H. Baabur-Cohen, A. Eldar-Boock, L. Omer, G. Tiram, S. Ferber, P. Ofek, D. Polyak, A. Scomparin, R. Satchi-Fainaro, *J. Control. Release* **2012**, *161*, 446–460.

[11] M. Calderón, M. A. Quadir, M. Strumia, R. Haag, *Biochimie* **2010**, *92*, 1242–1251.

[12] H. Ringsdorf, *J. Polym. Sci. Polym. Symp.* **2007**, *51*, 135–153.

[13] I. Ekladious, Y. L. Colson, M. W. Grinstaff, *Nat. Rev. Drug Discov.* **2019**, *18*, 273–294.

[14] I. Ozer, A. Tomak, H. M. Zareie, Y. Baran, V. Bulmus, *Biomacromolecules* **2017**, *18*, 2699–2710.

[15] Y. Hou, H. Lu, *Bioconjug. Chem.* **2019**, DOI 10.1021/acs.bioconjchem.9b00236.

[16] S. N. S. Alconcel, A. S. Baas, H. D. Maynard, *Polym. Chem.* **2011**, *2*, 1442.

[17] M. J. Webber, R. Langer, *Chem. Soc. Rev.* **2017**, *46*, 6600–6620.

[18] H.-J. Yoon, W.-D. Jang, *J. Mater. Chem.* **2010**, *20*, 211–222.

[19] G. R. Newkome, C. N. Moorefield, G. R. Baker, M. J. Saunders, S. H. Grossman, *Angew. Chemie Int. Ed. English* **1991**, *30*, 1178–1180.

[20] J. F. G. A. Jansen, E. M. M. de Brabander-van den Berg, E. W. Meijer, *Science* **1994**, *266*, 1226–1229.

[21] K. Kataoka, A. Harada, Y. Nagasaki, *Adv. Drug Deliv. Rev.* **2001**, *47*, 113–131.

[22] M. C. Lukowiak, B. N. S. Thota, R. Haag, *Biotechnol. Adv.* **2015**, *33*, 1327–1341.

[23] Y. Ma, Q. Mou, D. Wang, X. Zhu, D. Yan, *Theranostics* **2016**, *6*, 930–947.

[24] E. Gillies, J. Frechet, *Drug Discov. Today* **2005**, *10*, 35–43.

[25] D. A. Tomalia, J. M. J. Fréchet, *J. Polym. Sci. Part A Polym. Chem.* **2002**, *40*, 2719–2728.

[26] P. Kesharwani, K. Jain, N. K. Jain, *Prog. Polym. Sci.* **2014**, *39*, 268–307.

[27] G. T. Hermanson, in *Bioconjugate Tech.*, Elsevier, **2013**, pp. 351–386.

[28] C. Hawker, J. M. J. Fréchet, *J. Chem. Soc., Chem. Commun.* **1990**, 1010–1013.

[29] S. Svenson, A. S. Chauhan, *Nanomedicine* **2008**, *3*, 679–702.

[30] J. Khandare, M. Calderón, N. M. Dagia, R. Haag, *Chem. Soc. Rev.* **2012**, *41*, 2824–2848.

[31] O. Rolland, C.-O. Turrin, A.-M. Caminade, J.-P. Majoral, *New J. Chem.* **2009**, *33*, 1809.

[32] K. Fant, E. K. Esbjörner, A. Jenkins, M. C. Grossel, P. Lincoln, B. Nordén, *Mol. Pharm.* **2010**, *7*, 1734–1746.

[33] D. Wang, T. Imae, M. Miki, *J. Colloid Interface Sci.* **2007**, *306*, 222–227.

[34] A. Janaszewska, M. Studzian, J. F. Petersen, M. Ficker, V. Paolucci, J. B. Christensen, D. A. Tomalia, B. Klajnert-Maculewicz, *Colloids Surfaces B Biointerfaces* **2017**, *159*, 211–216.

[35] O. F. Khan, E. W. Zaia, S. Jhunjhunwala, W. Xue, W. Cai, D. S. Yun, C. M. Barnes, J. E. Dahlman, Y. Dong, J. M. Pelet, M. J. Webber, J. K. Tsosie, T. E. Jacks, R. Langer, D. G. Anderson, *Nano Lett.* **2015**, *15*, 3008–3016.

[36] O. L. Padilla De Jesús, H. R. Ihre, L. Gagne, J. M. J. Fréchet, F. C. Szoka, *Bioconjug. Chem.* **2002**, *13*, 453–461.

[37] S. J. Guillaudeu, M. E. Fox, Y. M. Haidar, E. E. Dy, F. C. Szoka, J. M. J. Fréchet, *Bioconjug. Chem.* **2008**, *19*, 461–469.

[38] R. H. Kienle, A. G. Hovey, *J. Am. Chem. Soc.* **1929**, *51*, 509–519.

[39] P. J. Flory, *J. Am. Chem. Soc.* **1952**, *74*, 2718–2723.

[40] B. I. Voit, A. Lederer, *Chem. Rev.* **2009**, *109*, 5924–73.

[41] Y. Zheng, S. Li, Z. Weng, C. Gao, *Chem. Soc. Rev.* **2015**, *44*, 4091–4130.

[42] F. Wurm, H. Frey, in *Polym. Sci. A Compr. Ref.*, Elsevier, **2012**, pp. 177–198.

[43] D. Wang, T. Zhao, X. Zhu, D. Yan, W. Wang, *Chem. Soc. Rev.* **2015**, *44*, 4023–4071.

[44] E. Žagar, M. Huskić, M. Žigon, *Macromol. Chem. Phys.* **2007**, *208*, 1379–1387.

[45] J. Twibanire, T. B. Grindley, *Polymers (Basel).* **2014**, *6*, 179–213.

[46] J. Liu, W. Huang, Y. Pang, X. Zhu, Y. Zhou, D. Yan, *Biomacromolecules* **2010**, *11*, 1564–1570.

[47] C. Chen, G. Liu, X. Liu, S. Pang, C. Zhu, L. Lv, J. Ji, *Polym. Chem.* **2011**, *2*, 1389.

[48] S. Abbina, S. Vappala, P. Kumar, E. M. J. Siren, C. C. La, U. Abbasi, D. E. Brooks, J. N. Kizhakkedathu, *J. Mater. Chem. B* **2017**, *5*, 9249–9277.

[49] S. R. Sandler, F. R. Berg, *J. Polym. Sci. Part A-1 Polym. Chem.* **1966**, *4*, 1253–1259.

[50] R. Tokar, P. Kubisa, S. Penczek, A. Dworak, *Macromolecules* **1994**, *27*, 320–322.

[51] A. Dworak, W. Walach, B. Trzebicka, *Macromol. Chem. Phys.* **1995**, *196*, 1963–1970.

[52] A. Sunder, R. Hanselmann, H. Frey, R. Mülhaupt, *Macromolecules* **1999**, *32*, 4240–4246.

[53] E. Moore, A. T. Zill, C. A. Anderson, A. R. Jochem, S. C. Zimmerman, C. S. Bonder, T. Kraus, H. Thissen, N. H. Voelcker, *Macromol. Chem. Phys.* **2016**, *217*, 2252–2261.

[54] K. Walker, J. Stumbé, R. Haag, *Polymers (Basel).* **2016**, *8*, 192.

[55] F. Du, S. Hönzke, F. Neumann, J. Keilitz, W. Chen, N. Ma, S. Hedtrich, R. Haag, *J. Control. Release* **2016**, *242*, 42–49.

[56] M. Unbehauen, E. Fleige, F. Paulus, B. Schemmer, S. Mecking, S. Moré, R. Haag, *Polymers (Basel).* **2017**, *9*, 316.

[57] F. Zabihi, S. Wieczorek, M. Dimde, S. Hedtrich, H. G. Börner, R. Haag, *J. Control. Release* **2016**, *242*, 35–41.

[58] F. Zabihi, P. Graff, F. Schumacher, B. Kleuser, S. Hedtrich, R. Haag, *Nanoscale* **2018**, *10*, 16848–16856.

[59] M. Dimde, D. Steinhilber, F. Neumann, Y. Li, F. Paulus, N. Ma, R. Haag, *Macromol. Biosci.* **2017**, *17*, 1600190.

[60] M. a. Quadir, M. R. Radowski, F. Kratz, K. Licha, P. Hauff, R. Haag, *J. Control. Release* **2008**, *132*, 289–294.

[61] E. Fleige, K. Achazi, K. Schaletzki, T. Triemer, R. Haag, *J. Control. Release* **2014**, *185*, 99–108.

[62] S. Stefani, I. N. Kurniasih, S. K. Sharma, C. Böttcher, P. Servin, R. Haag, *Polym. Chem.* **2016**, *7*, 887–898.

[63] N. Kamaly, B. Yameen, J. Wu, O. C. Farokhzad, *Chem. Rev.* **2016**, *116*, 2602–2663.

[64] R. Song, M. Murphy, C. Li, K. Ting, C. Soo, Z. Zheng, *Drug Des. Devel. Ther.* **2018**, *12*, 3117–3145.

[65] C. Caballero-George, Marin, Briceño, *Int. J. Nanomedicine* **2013**, 3071.

[66] M. Hirenkumar, S. Steven, *Polymers (Basel).* **2012**, *3*, 1–19.

[67] F. Danhier, E. Ansorena, J. M. Silva, R. Coco, A. Le Breton, V. Préat, *J. Control. Release* **2012**, *161*, 505–522.

[68] A. L. Sisson, D. Ekinci, A. Lendlein, *Polymer (Guildf).* **2013**, *54*, 4333–4350.

[69] S. H. Chang, H. J. Lee, S. Park, Y. Kim, B. Jeong, *Biomacromolecules* **2018**, *19*, 2302–2307.

[70] I. Manavitehrani, A. Fathi, H. Badr, S. Daly, A. Negahi Shirazi, F. Dehghani, *Polymers (Basel).* **2016**, *8*, 20.

[71] A. Díaz, R. Katsarava, J. Puiggalí, *Int. J. Mol. Sci.* **2014**, *15*, 7064–7123.

[72] N. Kumar, R. S. Langer, A. J. Domb, *Adv. Drug Deliv. Rev.* **2002**, *54*, 889–910.

[73] A. Basu, A. J. Domb, *Adv. Mater.* **2018**, *30*, 1–10.

[74] A. K. Andrianov, *J. Inorg. Organomet. Polym. Mater.* **2007**, *16*, 397–406.

[75] A. L. Baillargeon, K. Mequanint, *Biomed Res. Int.* **2014**, *2014*, 1–16.

[76] A. Linhardt, M. König, W. Schöfberger, O. Brüggemann, A. Andrianov, I. Teasdale, *Polymers (Basel).* **2016**, *8*, 161.

[77] B. D. Ulery, L. S. Nair, C. T. Laurencin, *J. Polym. Sci. Part B Polym. Phys.* **2011**, *49*, 832–864.

[78] S. Samanta, D. R. Bogdanowicz, H. H. Lu, J. T. Koberstein, *Macromolecules* **2016**, *49*, 1858–1864.

[79] U. Weiss, *Nature* **2008**, *454*, 427–427.

[80] C. G. Gahmberg, L. Valmu, S. Fagerholm, P. Kotovuori, E. Ihanus, L. Tian, T. Pessa-Morikawa, *Cell. Mol. Life Sci.* **1998**, *54*, 549–555.

[81] T. Lawrence, D. A. Willoughby, D. W. Gilroy, *Nat. Rev. Immunol.* **2002**, *2*, 787–795.

[82] P. Libby, *Nutr. Rev.* **2007**, *65*, 140–146.

[83] H. F. Langer, T. Chavakis, *J. Cell. Mol. Med.* **2009**, *13*, 1211–1220.

[84] H. Ulbrich, E. E. Eriksson, L. Lindbom, *Trends Pharmacol. Sci.* **2003**, *24*, 640–647.

[85] R. M. Rao, L. Yang, G. Garcia-Cardena, F. W. Luscinskas, *Circ. Res.* **2007**, *101*, 234–247.

[86] A. W. Greenberg, D. K. Brunk, D. A. Hammer, *Biophys. J.* **2000**, *79*, 2391–2402.

[87] D. Vestweber, J. E. Blanks, *Physiol. Rev.* **1999**, *79*, 181–213.

[88] U. Jung, K. Ley, *J. Immunol.* **1999**, *162*, 6755–62.

[89] J. B. Lowe, *Immunol. Rev.* **2002**, *186*, 19–36.

[90] N. S. Merle, S. E. Church, V. Fremeaux-Bacchi, L. T. Roumenina, *Front. Immunol.* **2015**, *6*, 1–30.

[91] D. R. Mathern, P. S. Heeger, *Clin. J. Am. Soc. Nephrol.* **2015**, *10*, 1636–1650.

[92] S. Kumar, B. K. Singh, P. Arya, S. Malhotra, R. Thimmulappa, A. K. Prasad, E. Van der Eycken, C. E. Olsen, A. L. DePass, S. Biswal, V. S. Parmarc, B. Ghosh, *Eur. J. Med. Chem.* **2011**, *46*, 5498–5511.

[93] S. W. Park, S. Banskota, P. Gurung, Y. J. Jin, H. Kang, C. L. Chaudhary, S. Y. Lee, B.-S. Jeong, J.-A. Kim, T. Nam, *Medchemcomm* **2018**, *9*, 1305–1310.

[94] R. P. McEver, K. L. Moore, R. D. Cummings, *J. Biol. Chem.* **1995**, *270*, 11025–8.

[95] W. D. Hanley, D. Wirtz, K. Kostantopoulos, *J. Cell Sci.* **2004**, *117*, 2503–2511.

[96] W. S. Somers, G. D. Shaw, R. T. Camphausen, *Cell* **2001**, *105*, 971.

[97] K. L. Moore, *Leuk. Lymphoma* **1998**, *29*, 1–15.

[98] S. R. Barthel, J. D. Gavino, L. Descheny, C. J. Dimitroff, *Expert Opin. Ther. Targets* **2007**, *11*, 1473–1491.

[99] R. E. Bruehl, F. Dasgupta, T. R. Katsumoto, J. H. Tan, C. R. Bertozzi, W. Spevak, D. J. Ahn, S. D. Rosen, J. O. Nagy, *Biochemistry* **2001**, *40*, 5964–5974.

[100] C. Fasting, C. A. Schalley, M. Weber, O. Seitz, S. Hecht, B. Koksch, J. Dernedde, C. Graf, E.-W. Knapp, R. Haag, *Angew. Chemie Int. Ed.* **2012**, *51*, 10472–10498.

[101] N. A. Raffler, J. Rivera-Nieves, K. Ley, *Drug Discov. Today Ther. Strateg.* **2005**, *2*, 213–220.

[102] L. Fu, M. Suflita, R. J. Linhardt, *Adv. Drug Deliv. Rev.* **2016**, *97*, 237–249.

[103] S. Mishra, K. Upadhaya, K. B. Mishra, A. K. Shukla, R. P. Tripathi, V. K. Tiwari, **2016**, pp. 307–361.

[104] Thorlacius, Vollmar, Seyfert, Vestweber, Menger, *Eur. J. Clin. Invest.* **2000**, *30*, 804–810.

[105] P. Driguez, P. Potier, P. Trouilleux, *Nat. Prod. Rep.* **2014**, *31*, 980.

[106] H. Türk, R. Haag, S. Alban, *Bioconjug. Chem.* **2004**, *15*, 162–167.

[107] I. Papp, J. Dernedde, S. Enders, R. Haag, *Chem. Commun.* **2008**, 5851.

[108] S. Enders, G. Bernhard, A. Zakrzewicz, R. Tauber, *Biochim. Biophys. Acta - Gen. Subj.* **2007**, *1770*, 1441–1449.

[109] M. Weinhart, D. Gröger, S. Enders, J. Dernedde, R. Haag, *Biomacromolecules* **2011**, *12*, 2502–2511.

[110] J. Dernedde, A. Rausch, M. Weinhart, S. Enders, R. Tauber, K. Licha, M. Schirner, U. Zugel, A. von Bonin, R. Haag, *Proc. Natl. Acad. Sci.* **2010**, *107*, 19679–19684.

[111] M. Weinhart, D. Gröger, S. Enders, S. B. Riese, J. Dernedde, R. K. Kainthan, D. E. Brooks, R. Haag, *Macromol. Biosci.* **2011**, *11*, 1088–1098.

[112] F. Paulus, R. Schulze, D. Steinhilber, M. Zieringer, I. Steinke, P. Welker, K. Licha, S. Wedepohl, J. Dernedde, R. Haag, *Macromol. Biosci.* **2014**, *14*, 643–654.

[113] K. Pant, D. Gröger, R. Bergmann, J. Pietzsch, J. Steinbach, B. Graham, L. Spiccia, F. Berthon, B. Czarny, L. Devel, V. Dive, H. Stephanet, R. Haag, *Bioconjug. Chem.* **2015**, *26*, 906–918.

[114] S. Reimann, D. Gröger, C. Kühne, S. B. Riese, J. Dernedde, R. Haag, *Adv. Healthc. Mater.* **2015**, *4*, 2154–2162.

[115] R. L. Siegel, K. D. Miller, A. Jemal, *CA. Cancer J. Clin.* **2019**, *69*, 7–34.

[116] F. Bray, J. Ferlay, I. Soerjomataram, R. L. Siegel, L. A. Torre, A. Jemal, *CA. Cancer J. Clin.* **2018**, *68*, 394–424.

[117] M. Sechi, V. Sanna, N. Pala, *Int. J. Nanomedicine* **2014**, *9*, 467.

[118] D. Hanahan, R. A. Weinberg, *Cell* **2000**, *100*, 57–70.

[119] D. Hanahan, R. A. Weinberg, *Cell* **2011**, *144*, 646–74.

[120] I. Kareva, P. Hahnfeldt, *Cancer Res.* **2013**, *73*, 2737–2742.

[121] Y. Kato, S. Ozawa, C. Miyamoto, Y. Maehata, A. Suzuki, T. Maeda, Y. Baba, *Cancer Cell Int.* **2013**, *13*, 89.

[122] V. Huber, C. Camisaschi, A. Berzi, S. Ferro, L. Lugini, T. Triulzi, A. Tuccitto, E. Tagliabue, C. Castelli, L. Rivoltini, *Semin. Cancer Biol.* **2017**, *43*, 74–89.

[123] D. Trachootham, J. Alexandre, P. Huang, *Nat. Rev. Drug Discov.* **2009**, *8*, 579–591.

[124] L. M. Coussens, Z. Werb, *Nature* **2002**, *420*, 860–867.

[125] D. Polyak, A. Eldar-Boock, H. Baabur-Cohen, R. Satchi-Fainaro, *Polym. Adv. Technol.* **2013**, *24*, 777–790.

[126] N. Bertrand, J. Wu, X. Xu, N. Kamaly, O. C. Farokhzad, *Adv. Drug Deliv. Rev.* **2014**, *66*, 2–25.

[127] F. Danhier, O. Feron, V. Préat, *J. Control. Release* **2010**, *148*, 135–146.

[128] I. Vhora, S. Patil, P. Bhatt, R. Gandhi, D. Baradia, A. Misra, *Ther. Deliv.* **2014**, *5*, 1007–1024.

[129] B. Varghese, E. Vlashi, W. Xia, W. Ayala Lopez, C. M. Paulos, J. Reddy, L. C. Xu, P. S. Low, *Mol. Pharm.* **2014**, *11*, 3609–3616.

[130] E. Nogueira, A. C. Gomes, A. Preto, A. Cavaco-Paulo, *Nanomedicine Nanotechnology, Biol. Med.* **2016**, *12*, 1113–1126.

[131] S. Wang, C. Zhao, P. Liu, Z. Wang, J. Ding, W. Zhou, *RSC Adv.* **2018**, *8*, 444–453.

[132] Y. Matsumura, H. Maeda, *Cancer Res.* **1986**, *46*, 6387–92.

[133] H. Maeda, *Adv. Drug Deliv. Rev.* **2015**, *91*, 3–6.

[134] R. Haag, F. Kratz, *Angew. Chemie Int. Ed.* **2006**, *45*, 1198–1215.

[135] V. Torchilin, *Adv. Drug Deliv. Rev.* **2011**, *63*, 131–135.

[136] E. Fleige, M. A. Quadir, R. Haag, *Adv. Drug Deliv. Rev.* **2012**, *64*, 866–884.

[137] S. Mura, J. Nicolas, P. Couvreur, *Nat. Mater.* **2013**, *12*, 991–1003.

[138] M. Karimi, M. Eslami, P. Sahandi-Zangabad, F. Mirab, N. Farajisafiloo, Z. Shafaei, D. Ghosh, M. Bozorgomid, F. Dashkhaneh, M. R. Hamblin, *Wiley Interdiscip. Rev. Nanomedicine Nanobiotechnology* **2016**, *8*, 696–716.

[139] A. Landarani-Isfahani, M. Moghadam, S. Mohammadi, M. Royvaran, N. Moshtael-Arani, S. Rezaei, S. Tangestaninejad, V. Mirkhani, I. Mohammadpoor-Baltork, *Langmuir* **2017**, *33*, 8503–8515.

[140] X. Zhang, D. Li, J. Huang, K. Ou, B. Yan, F. Shi, J. Zhang, J. Zhang, J. Pang, Y. Kang, et al., *J. Mater. Chem. B* **2019**, *7*, 251–264.

[141] S. S. Kelkar, T. M. Reineke, *Bioconjug. Chem.* **2011**, *22*, 1879–1903.

[142] X. Wang, Y. Yang, Y. Zhuang, P. Gao, F. Yang, H. Shen, H. Guo, D. Wu, *Biomacromolecules* **2016**, *17*, 2920–2929.

[143] M. Calderón, P. Welker, K. Licha, I. Fichtner, R. Graeser, R. Haag, F. Kratz, *J. Control. Release* **2011**, *151*, 295–301.

[144] A. Sousa-Herves, P. Würfel, N. Wegner, J. Khandare, K. Licha, R. Haag, P. Welker, M. Calderón, *Nanoscale* **2015**, *7*, 3923–3932.

[145] F. Kratz, I. A. Müller, C. Ryppa, A. Warnecke, *ChemMedChem* **2008**, *3*, 20–53.

[146] T. Ji, Y. Zhao, Y. Ding, J. Wang, R. Zhao, J. Lang, H. Qin, X. Liu, J. Shi, N. Tao, Z. Qin, G. Nie, Y. Zhao, *Angew. Chemie Int. Ed.* **2016**, *55*, 1050–1055.

[147] M. Calderón, R. Graeser, F. Kratz, R. Haag, *Bioorg. Med. Chem. Lett.* **2009**, *19*, 3725–3728.

[148] F. Fouladi, K. J. Steffen, S. Mallik, *Bioconjug. Chem.* **2017**, *28*, 857–868.

[149] W. Sun, W. Ji, Q. Hu, J. Yu, C. Wang, C. Qian, G. Hochu, Z. Gu, *Biomaterials* **2016**, *96*, 1–10.

[150] Z. Zhang, Y. Zhou, Z. Zhou, Y. Piao, N. Kalva, X. Liu, J. Tang, Y. Shen, *Polym. Chem.* **2018**, *9*, 438–449.

[151] S. Saxena, M. Jayakannan, *J. Polym. Sci. Part A Polym. Chem.* **2016**, *54*, 3279–3293.

[152] G. Filomeni, G. Rotilio, M. R. Ciriolo, *Biochem. Pharmacol.* **2002**, *64*, 1057–1064.

[153] A. Bansal, M. C. Simon, *J. Cell Biol.* **2018**, *217*, 2291–2298.

[154] J. F. Quinn, M. R. Whittaker, T. P. Davis, *Polym. Chem.* **2017**, *8*, 97–126.

[155] H. Wen, H. Dong, J. Liu, A. Shen, Y. Li, D. Shi, *J. Mater. Chem. B* **2016**, *4*, 7859–7869.

[156] M. Cai, M. Ye, X. Shang, H. Sun, M. Liu, H. Sun, Z. Ma, H. Zhu, *RSC Adv.* **2015**, *5*, 92292–

92302.

[157] Y. Zhong, M. Dimde, D. Stöbener, F. Meng, C. Deng, Z. Zhong, R. Haag, *ACS Appl. Mater. Interfaces* **2016**, *8*, 27530–27538.

[158] N. Rades, K. Achazi, M. Qiu, C. Deng, R. Haag, Z. Zhong, K. Licha, *J. Control. Release* **2019**, *300*, 13–21.

7 Appendix

7.1 List of abbreviations

AP	alternative pathway
Au NP	gold nanoparticles
CAMs	cell adhesion molecules
CP	classical pathway
DB	degree of branching
DDS	drug delivery systems
Doxo	doxorubicin
dPG	dendritic poly(glycerol)
dPGS	dendritic poly(glycerol) sulfate
ECM	extracellular matrix
EGF	epidermal growth factor domain
EPR	enhanced permeation and retention effect
eq.	equivalent
FDA	Food and Drug Administration
GAG	glycosaminoglycan
GEM	gemcitabine
GSH	glutathione
GSSG	glutathione-disulfide
h	hour
hPG	hyperbranched poly(glycerol)
hPG-co-PCL	hyperbranched poly(glycerol-co-caprolactone)
hPG-co-PCLS	hyperbranched poly(glycerol-co-caprolactone) sulfate
HPLC	gigh-performance liquid chromatography
ICAMs	intercellular adhesion molecules
Ig	immunoglobulin
IL-1	interleukin-1
JCAMs	junction adhesion molecules
kDa	kilo Dalton
LP	lectin pathway
MAC	membrane-attack complex
MMAE	monomethyl auristatin E

MMPs	matrix metalloproteinases
MTX	methotrexate
NIR	near infrared
NMR	nuclear magnetic resonance
PAMAM	poly(amido amine)
PB	phosphate buffer
PBS	poly(butylene succinate)
PCL	poly(caprolactone)
PDI	polydispersity index
PEG	poly(ethylene glycol)
PEO	poly(ethylene oxide)
PGA	poly(glycolide)
PLA	poly(lactide)
PLGA	poly(lactide-co-glycolide)
PPI	poly(propylene imine)
ppm	parts per million
PSGL-1	P-selectin glycoprotein ligand-1
PXT	paclitaxel
quant.	quantitative
RGD	arginylglycylaspartic acid
ROMB	ring opening multibranching polymerization
ROS	reactive oxygen species
RP-HPLC	reversed phase-high performance liquid chromatography
sLe^a	sialyl Lewis A
sLe^x	sialyl Lewis x
SPR	surface plasmon resonance
TLC	thin layer chromatography
TNF-α	tumor necrosis factor alpha
UFH	unfractionated heparin
VCAMs	vascular adhesion molecules

7.2 List of publications (journals, posters, patents)

7.2.1 List of Publications

[1] **M. Ferraro**[§], K. Silberreis[§], E. Mohammadifar, F. Neumann, J. Dernedde, R. Haag, Biodegradable Polyglycerol Sulfates Exhibit Promising Features for Anti-inflammatory Applications. *Biomacromolecules,* **2018***, 19(12),* 4524–4533.
DOI: 10.1021/acs.biomac.8b01100

[2] P. Ray, **M. Ferraro**, R. Haag, M. Quadir, Dendritic Polyglycerol-derived nano-architectures as delivery platforms of gemcitabine for pancreatic cancer. *Macromolecular Bioscience*, accepted

7.2.2 List of Patent Applications

R. Haag, E. Mohammadifar, **M. Ferraro,** F. Zabihi, M. Adeli, November 2017, European patent application. *Method for manufacturing a hyperbranched polyester polyol derivative*. EP17201626.3

7.2.3 List of Poster Presentations

M. Ferraro, E. Mohammadifar, K. Silberreis, F. Neumann, J. Dernedde, R. Haag. Development of sulfated biodegradable polymers with anti-inflammatory potential. BCS & ChiP 2018, Berlin, Germany, 2018.

M. Ferraro, E. Mohammadifar, K. Silberreis, F. Neumann, J. Dernedde, R. Haag. Development of sulfated biodegradable polymers with anti-inflammatory potential. Biodendrimer 2018: 6th International Symposium on Biomedical Applications of Dendrimers, Urbino, Italy, 2018.

7.2.4 List of Oral Presentations

M. Ferraro, R. Haag. Core-multishell architectures from epoxide monomers for drug delivery. MacroBio Summer School 2016, Berlin, Germany, 2016.

M. Ferraro, R. Haag. Sulfated Dendritic Polymers with high Anti-inflammatory Potential. The FUB-HUJI GAGs Workshop: Synthesis to Applications, Hebrew University of Jerusalem, Israel, 2018.

7.3 Curriculum vitae